AN EXPERIMENTAL STUDY OF THE SURFACE DISTRIBUTION OF FILLER MATERIAL IN PAPER

by

ANDREW SERLES

B.A.Sc., Queen's University, Canada, 2010

A THESIS SUBMITTED IN PARTIAL FULFILLMENT OF THE REQUIREMENTS FOR THE DEGREE OF

MASTER OF APPLIED SCIENCE

in

THE FACULTY OF GRADUATE STUDIES

(Mechanical Engineering)

THE UNIVERISTY OF BRITISH COLUMBIA
(Vancouver)

October 2012

ABSTRACT

A series of experiments were conducted to observe the effect of different pulp suspension and formation characteristics on the variation in filler concentration on the surface of paper. Hand sheet samples were formed in a laboratory apparatus. The surface distribution of two types of filler material was investigated: Precipitated Calcium Carbonate ($CaCO_3$) and Kaolin Clay ($Al_2Si_2O_5(OH)_4$). The effect of retention aids, dewatering rate, and forming fabric geometry on filler distribution was tested.

The analysis was focused on the variation in surface filler concentrations on the scale of individual strands of the forming fabric. The procedure involved locating areas of interest in the samples, particularly the area of paper formed over knuckles, threads, and openings in the fabric, at which point the sample was analysed with Energy Dispersive X-Ray Spectroscopy and image analysis techniques to determine relative filler concentrations.

In samples formed by gravity and vacuum drainage, Kaolin displayed a significantly greater variation in local surface filler concentration than PCC, though the difference was reduced under vacuum drainage conditions. This effect is attributed to the electrostatic attraction between PCC and pulp fibres in contrast with the repulsion felt by Kaolin filler. The attraction resists the distributing forces of the flow at low drainage velocities but the bonds are broken by large shear forces. The distribution on the top side of the paper was comparable between the filler types, due to the more uniform flow field at a distance from the forming fabric. Vacuum drainage increased the spatial variation of both fillers by a similar amount.

It was found that under vacuum drainage, retention aids did not improve filler uniformity on the wire side. However, on the top side of the paper, a moderate reduction in spatial variation was observed. Additionally, on the wire side of samples made with gravity drainage, it was found that the addition of retention aids produced a significant improvement in the uniformity of the filler material. Finally, it was found that a finer forming fabric improved the uniformity of filler distribution.

TABLE OF CONTENTS

LIST OF TABLES

LIST OF FIGURES

ACKNOWLEDGEMENTS

CHAPTER 1 – INTRODUCTION AND BACKGROUND

1.1   Introduction to Papermaking

Paper is made with a multitude of components, the concentrations of which can be varied to control the properties of the final product. The type of wood pulp used in the process will dramatically affect the quality of the final product. There are multiple ways to process raw wood into pulp, each with various advantages and disadvantages. Some examples include: mechanical pulping, thermo-mechanical pulping, and chemical pulping. Lower quality pulps are cheaper to produce and are used in cheaper paper, such as newsprint, while more refined pulps are used to make high end printing paper [1, 2]. In addition to the wood pulp fibres and water, filler material is often added to the pulp slurry. Filler affects the strength, opacity, smoothness, printability and brightness of the final product, as well as being a less expensive substitute for wood pulp. Some typical filler materials used in industry are calcium carbonate, clay, starches, and titanium dioxide [3, 4]. Other chemicals are added to control various portions of the papermaking process. Some examples include: retention aids, drainage aids, flocculants, and pH controls. The entire mixture is often referred to as a pulp slurry or pulp suspension, and the balance of all the components is a large factor in determining the features of the final paper product [5].

The modern paper machine is comprised of five unique sections: the approach section, the forming section, the pressing section, the drying section, and the finishing section [6]. A rough schematic of the entire machine is shown in Figure 1.
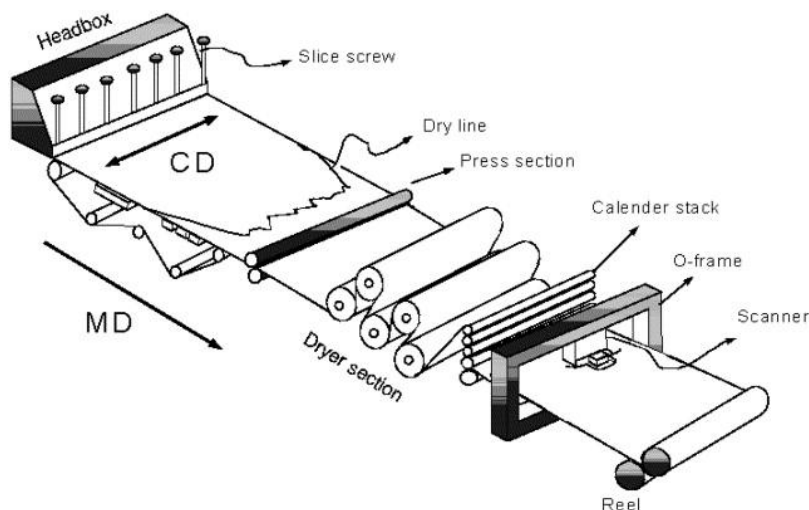
Figure 1: Schematic of Fourdrinier Papermaking Machine [7]

The first portion of the paper machine is called the approach section. The approach section contains the machinery responsible for mixing the required pulp suspension and the uniform delivery of this suspension to the next section. The first stage of the approach is stock preparation, where the pulp is screened and chemicals are added. Next, in the stock approach systems, the suspension is screened further and white water is added to dilute the suspension to the desired consistency. Finally the pulp is delivered to the headbox, a device which transfers the suspension to the next stage of the paper machine as a uniform pressurized jet [1].

The next section of the machine is called the forming section. This is where the dewatering process begins and the paper starts to take shape. At the beginning of the forming section the consistency of the pulp suspension is 0.5%. There are different types of formers which are chosen based on the desired properties of the paper. The simplest type, and the one most like the experimental setup used for this research is the Fourdrinier former. With this machine, a finely woven continuous synthetic weave called the forming fabric, is circulated like a conveyor belt under high tension. The jet of pulp suspension from the headbox impinges on the forming fabric, which traps the solid material. Throughout the length of the forming section, various devices, such as the wet and dry suction boxes and foils, are located under the top side of the forming fabric to remove water from the wet paper web. These dewatering devices are designed to maximize water removal while minimizing the disturbance to the paper [8, 9]. Another type of former design is the twin wire former, which removes water from both sides of the paper. This is done by impinging the jet from the headbox between two converging fabrics. Since water is removed from both sides of the paper in a twin wire former, the paper properties are almost symmetric about the centre of the sheet [1]. The paper forms a continuous sheet in the forming section and leaves with a consistency of about 20% [6].

The next section is the press section, where more water is removed from the wet paper web. The press section uses the compression of the paper to extract water. The wet web is fed through two rolls covered in felt. As the paper is pulled through the compression, water is squeezed out of the paper and absorbed by the felt on the rolls. Water is also removed with a single roll by turning the direction the paper is travelling through an angle around a roller. The tension forces out water which is again absorbed by the felt roll coverings. The arrangements of the rollers in the press section can be very convoluted and the design depends on the type of paper and the intended machine speed [6].

The paper web leaving the press section will have consistency between 35 and 50% as it continues to the dryer section [10]. The drying section uses heat to evaporate additional water and is the most expensive portion of the paper machine due to the energy costs. The paper must be dried to a consistency of 90 percent before it can be processed in the final section. The drying section removes water through a combination of conduction and convection effects. The paper is passed over large heated drums and lightly held onto the surface with a permeable dryer fabric. The drums evaporate water by conduction and the process is accelerated by blowing hot air over the paper web to increase convection. The paper is passed to the final portion of the machine at a consistency of 90 - 97 percent [6].

The final stages of the paper machine involve calendering, finishing and winding. The calendering process is designed to make the paper thinner and smoother by employing a similar compression process to that used in the pressing section. The calendar rolls are usually made of hardened iron, ground to low roughness levels. The finishing aspect of the process involves treating the surface of the paper with chemicals, such as starch, to increase the overall strength, opacity, smoothness, and brightness of the final product. Finally the paper is wound around a spool, much like thread. The paper machine ejects the paper in an enormous, continuous sheet. The sheet is wound onto a roll and severed at a predetermined size. Once wound, the rolls can be cut to size and transported [6].

1.2   The Forming Section and Suction Boxes

The forming section is the first stage of the dewatering process. From a fluid dynamics standpoint, this section of the paper machine is the most interesting. Since the consistency is the lowest of all the sections at 0.5%, the liquid and solid portions of the pulp suspension have the most freedom of movement. At the beginning of the forming section, the suspension is dilute enough that gravity drainage takes place. Water drains from the pulp suspension, through the forming fabric, under its own weight and with the help of light pressure pulses developed by stationary dewatering elements, called foils [11]. The forming fabric is a woven web of plastic threads. The weaving pattern can be quite complex and involve multiple layers – considerable design goes into the construction of the geometry. Different weaves are used to either reduce or promote a wide range of formation characteristics, including: fibre retention, resistance to drainage, formation uniformity, and minimization of wire mark

[12]. Above a consistency of 5 - 7%, gravity will not remove any additional water from the wet web, so an applied pressure drop is employed to continue the water removal process [11]. This is done in several ways, including foils, vacuum boxes (also called suction boxes), and the suction boxes on the couch roll.

The suction box is a device located beneath the forming fabric that uses a vacuum to draw water from the pulp mat. The boxes have a perforated or slotted upper surface that allows for water to flow from the paper mat and into the box. As the fabric moves over a vacuum box, a suction pulse is applied to the wet paper web. Water is removed by creating a vacuum in the boxes and the difference in pressure between the ambient air and the vacuum draws water out of the paper and into the suction box. A schematic of a portion of the forming section with a magnified suction box is shown in Figure 2.
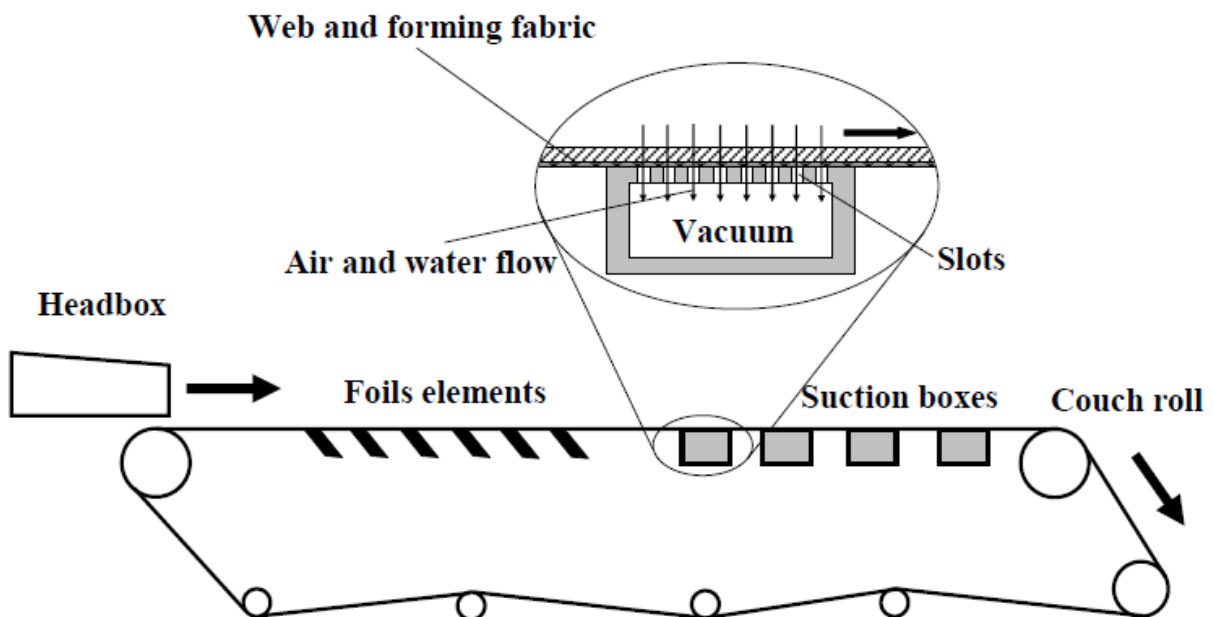
Figure 2: Magnified schematic of a vacuum box [13]

The gauge pressure created by the suction boxes is typically between -15 and -40 kPa, but can be as low as -65 kPa on extremely fast moving paper machines [6, 13]. The suction box area of the forming section increases the consistency of the wet web from between 4 and 10% to 20%. Several parameters of the suction boxes affect the dewatering of the pulp mat. It has been determined that the most important factor for attaining higher consistency is suction pressure, followed by suction time. The action of the paper moving over and off of a suction box creates a pressure pulse. Lower pulse frequencies are preferable at lower suction pressures, so the pulse frequency must be adapted to the suction pressure [14]. The basis weight of the paper (g/m^2) was found to reduce the drainage rate by suction.

Consequently, at higher basis weights, a longer suction time is required to achieve a similar dryness level. The same is reported for the presence of fines and filler material. In both cases, the specific filtration resistance of the web is increased, reducing drainage rate. This is explained by reduced permeability of the wet web due to filling of the area between fibres in the fibre network. Other factors that affect the performance of the suction box are the pulp type, freeness, consistency, and temperature [8].

In the forming section, the majority of the water removed is considered "free water", that is, water that is contained between fibres in the pulp mat. In later sections, such as the drying section, the water is evaporated from within layers and the cells of the actual pulp fibres. This is why the water is much more easily removed in the forming section. Three mechanisms rule the removal of water by suction boxes: web compressions, water displacement by air flow, and rewetting. As the saturated wet web passes over a suction box, it experiences a suction pulse that compresses the web. This compression pushes water out, thus the effectiveness of the suction box is linked to the compressibility of the web [13]. Secondly, water is displaced by air flowing through the web. The air motion is due to the pressure differential between the ambient air and the suction box. For the air to penetrate the initially water saturated wet web and start flowing from one side of the paper to the other, the applied suction pressure must exceed the capillary pressure of the water between the pulp fibres. As the paper leaves the suction box, the applied pressure is removed, allowing the pulp mat to expand again. This expansion pulls water that had been retained by the forming fabric back into the paper, rewetting the paper. The combination of these three mechanisms determines the overall effectiveness of the suction box [13, 15].

1.3   Filler Material and Retention Aids

The addition of filler material to paper improves quality and certain aspects of formation, as well as providing economic savings by replacing wood pulp. This has spurred an industry trend to increase the filler content in pulp slurries. In terms of the finished product, addition of filler material reduces surface roughness, and increases the opacity, smoothness, and brightness of the paper [16]. There are drawbacks to increased filler loading that still need to be addressed, which have created limitations on the amount of filler that can be added to pulp slurries; particularly, that the permeability of the wet web decreases with filler content above a certain threshold, reducing drainage [9, 17].

Increasing the amount of filler material in paper provides several economic benefits. Once the free water has been drained from the wet web, additional drying becomes exponentially more difficult as the remaining water is contained in and around the cells of the wood pulp. It has been reported that the drying section consumes 60% of the total energy used to operate the paper machine, but removes as little as 1% of the total water [18, 19]. Thus any way to increase the solid content heading into the drying section can dramatically decrease operational costs. One way to do this is to increase the filler content in the paper. It has been found that paper with higher filler concentrations can be dried more quickly and the solid content of the paper leaving the pressing section is increased. Additionally, mineral fillers tend to be less expensive than wood pulp fibres by weight, so an increase in filler content reduces the cost of the raw materials [16].

One of the most commonly used filler materials is Calcium Carbonate ($CaCO_3$). There are two main types of Calcium Carbonate: Ground Calcium Carbonate (GCC) and Precipitated Calcium Carbonate (PCC). GCC is made by grinding naturally occurring calcium carbonate materials, usually either limestone or marble. Since GCC makes use of natural ground up minerals, the particles tend to have a random shape and size, and the product contains impurities and contaminants [20]. These features are undesirable in papermaking, where consistent, homogeneous materials are preferred. A SEM image of GCC particles is shown in Figure 3.

Figure 3: Image of GCC particles [21]

Precipitated Calcium Carbonate is manufactured. The size and shape of the particles can be controlled with the manufacturing method and are usually rhombehedral (barrel shaped), scalenohedral (rosette),

or acicular (needle). Scalenohedral PCC (S-PCC) is the most common particle shape used in paper filler. An example of the particles can be seen in Figure 4.
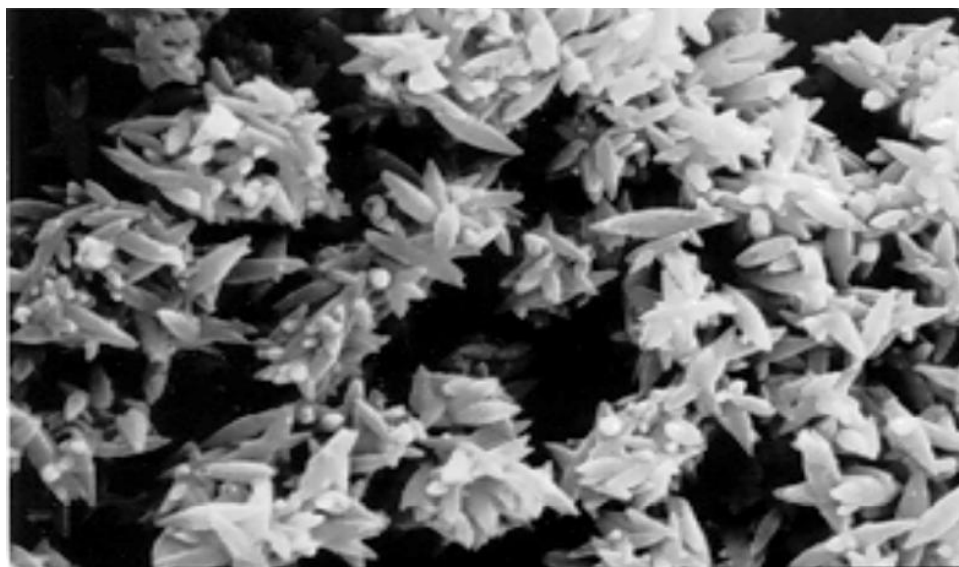
Figure 4: Scalenohedral PCC particles [21]

PCC provides higher opacity at lower filler loadings than GCC, as well as higher brightness and light scattering coefficients, while GCC provides higher strength and easier drainage. The optical properties have made PCC the preferred filler choice [22].

A second widely used filler material is clay. There are several different types of clay used in papermaking, the most common of which is a naturally occurring compound called Kaolin ($Al_2Si_2O_5(OH)_5$) [23]. Kaolin clay has the same drawbacks as other natural filler materials – random particle shape and the presence of impurities. However, it exhibits many of the same filler properties that make Calcium Carbonate appealing: white colour, fine particle size, easily dispersible in water and inert at medium PH levels. Kaolin does not match the optical properties of PCC but is often used for its low cost [17, 23].

One of the major properties of the filler material affecting the final paper product is its surface charge. It is well documented that wood pulp fibres in a pulp suspension are anionic, so the surface charge of the filler material will determined whether it is attracted to or repelled by the pulp fibres [24, 25, 26]. Cationic filler particles are attracted to the wood pulp and anionic particles are repelled. It has been shown that aqueous suspensions of GCC and PCC both tend to be cationic in distilled water under the same conditions [27]. Kaolin is anionic in distilled water and is thus repelled by the wood fibres [28]. Additionally, the charge of the particles affects their tendency to aggregate. When the charge is near neutral, PCC dispersed in water is unstable and will tend to aggregate into larger particles. However, if

sufficiently charged, the particles will repel each other and aggregates will not form. These charge properties all have an effect on the retention of the wet web [24, 29].

Retention is a term used to describe how much of the initial solid material in the pulp suspension remains in the final paper product. This value is important since it represents how much solid material must be used initially to form paper of the desired basis weight. Obviously, higher retention is preferred. Higher retention values translate into fewer raw materials required and consequently cost savings. The retention during sheet formation is affected by many properties of the papermaking process, including: filler type, intensity and frequency of pressure pulses (applied suction), chemical retention aids, basis weight, forming fabric geometry and machine speed [30, 31]. The main elements in the pulp suspension are of varying sizes, and consequently they are retained by different mechanisms. Wood pulp fibres normally range from 0.5 to 2 mm, wood fines, which are shattered pieces of fibres, are about $16 - 25$ μm long and filler particles are on the order of 0.1 to 10 μm in diameter [32, 33, 34]. The larger pulp fibres are retained by the strands of the forming fabric, creating the web that allows for the mechanical entrapment of the larger fines [32]. The very small filler and fine particles are retained by a combination of adsorption, filtration, sedimentation and flocculation; these particles are too small to be retained by the forming fabric [35, 36, 37]. Chemical retention aids are used to increase the retention of fines and filler material.

Retention aids help to retain small particles in two main ways: through the deposition of filler particles on fibres by charge modification, and molecular bridging of the filler to the pulp fibres [38, 35, 27]. Both mechanisms work by increasing flocculation in the suspension [39]. In molecular bridging, an adsorbed polymer creates a link between particles. Generally, this is a high molecular weight and low charge density cationic polymer. Charge modifying retention aids work by increasing the electrostatic attraction between the fines and pulp fibres. In general, it is the highly charged cationic polyelectrolytes that promote deposition of filler on fibres via charge modification [29, 38, 35, 39, 30]. Many different types of retention aids are used in paper making; it is an area of considerable ongoing research. Some common types include polyacrylamide (PAM), polyethylenimine (PEI), and polyethyleneoxide (PEO) [39]. Charge modifying retention aids form what are called "soft flocs". These types of flocculations are usually small and compact but are easily broken by turbulence. Retention aids that operate through bridging tend to form "hard flocs". Hard flocs tend to be larger and looser bonds that show some resistance to turbulence [40]. One of the main issues with soft flocs is the susceptibility of the attachment to high shear forces. The electrostatic attachment of the filler particles to the pulp fibres is

not strong enough to resist large hydrodynamic forces [35, 40]. Consequently the effectiveness of different types of retention aids is dependent on the specifications of the paper machine. Faster moving machines with large pressure pulses will exert larger shear forces on the flocculations than their slower counterparts.

It has been found that the majority of the bonding between filler and fines occurs in the headbox of the paper machine. The mixing caused by the removal of water by drainage has a significantly smaller frequency of creating bonds between fillers and fibres [37]. Thus, with bonds that are resistant to the drainage shear forces, the filler material should be uniformly distributed along the wood pulp fibres, since most bonding occurred in the headbox where the suspension was thoroughly mixed. However, it is anticipated that in cases where the bonds are not resistant to shear forces, a distribution pattern in the concentration of the filler will be visible in the paper. The filler material should be bound to pulp fibres in a higher concentration in the areas of high flow volume, because of the increased probabilistic deposition of the filler material onto the pulp fibres.

1.4   Filler Distribution

When referring to the dimensions of a sheet of paper, it is the standard to label the axis through the thickness of the paper the Z direction, and axes along the length and width the X and Y directions. These axes are commonly referred to as the cross sectional, cross machine, and machine directions, respectively. A schematic of the axes is shown in Figure 5.
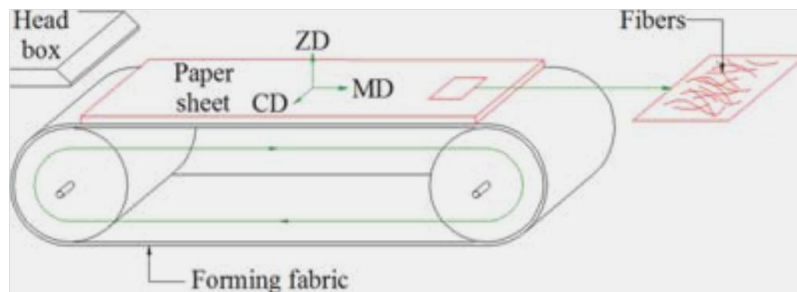
Figure 5: Schematic of the forming sections showing the axes used to describe a paper sample [41]

 Due to certain properties of the paper making components and process, non uniformities in the distribution of the filler material in the X, Y, and Z directions of the paper develop [41]. The filler distribution dramatically affects the properties of the final product, so paper made for different

9

purposes requires different distribution patterns. For example, copy paper requires surface filler content lower than the average filler content to reduce dusting; while supercalendered paper, inkjet printing paper and coated paper require high concentrations of filler material on the surface but do not need similar levels in the centre [3, 42, 43].

In general, additional filler material increases the surface quality of the paper by decreasing roughness and increasing brightness. It has also been seen that paper strength increases at constant filler content when the concentration on the surface increased [44]. Additionally, when the filler material is concentrated on the surfaces, the bending stiffness was reduced. Stiffness increases when filler is concentrated towards the centre of the paper thickness [45]. An extremely important property of filler distribution is its effect on printing applications. High surface filler concentrations reduce paper roughness, creating a desirable printing surface [41]. The small filler particles work to fill any large pores on the paper surface, which are the main cause of missing print in rotogravure printing [46]. Additionally, paper is made with the intent of reducing its "ink strike through", the term used to describe the penetration of ink into the paper. The worst case is when the ink penetrates the thickness of the paper and bleeds onto the opposing side. Good ink strike through (minimal penetration) is dependent on the surface makeup of the paper, since the ink is printed onto the paper surface. High surface filler concentration is essential to improving strike through [47]. In addition to adequate surface concentration, the uniformity of the surface filler material is important. The filler must be distributed evenly across the surface to prevent misprints and ink penetration in localised areas.

Filler distribution in the Z direction of the paper has been studied extensively [48, 49, 41] and it has been shown that the dewatering conditions are mainly responsible for the migration of filler and fines [3, 43, 50]. Z directional filler distributions tend to be characteristic of the type of former used to make the paper, due to the distinct dewatering techniques employed in different formers. In a Fourdrinier paper machine, where the water is drained through the forming fabric on one side of the paper the two sides of the paper have very different Z-direction filler distributions. The pressure pulses from the suction boxes remove filler material from the wire side of the paper, so the top side of the paper will have a higher concentration [41, 43]. In hybrid formers, 20 to 30 % of the drainage is done through the top side of the paper. This increases symmetry between the two sides but results in a higher concentration of filler in the centre of the paper than the surfaces [42, 43]. In a twin wire former where water is removed from both sides of the paper simultaneously, the filler distribution is almost symmetric, as would be expected. The concentration profile is controlled by the applied suction. Finally, with paper samples

made in hand sheet formers – a common practice in laboratory experiments, filler is concentrated towards the wire side. This can be explained by the relatively low drainage rate (in comparison to paper machine formers) and the single sustained pressure pulse used to make hand sheets [51, 52].

Moderate work has been done to investigate the uniformity of paper surface material and the effect on printing as well as the Z-direction filler distribution towards the surface [46, 47]. However, existing work on the distribution of filler material on the surface of the paper is limited, and work on the surface distribution caused by the forming fabric geometry has not been done. It is known that the electrostatic attraction between cationic filler particles and pulp fibres has a weak resistance to hydrodynamic forces [40, 3, 50]. It is also known that although most retention occurs due to electrostatic bonding in the headbox, a portion of the deposition of fines and fillers onto the pulp fibres occurs due to mechanical entrapment during the drainage of white water from the wet mat [37]. It has been experimentally and numerically shown that the geometry of the forming fabric has an influence on the z-component of the drainage velocity through the forming fabric [53, 54]. In the XY plane, at a distance of 0.25d from the forming fabric (where d is the diameter of a fabric strand), H. Peng was able to experimentally show that the Z-direction flow velocity differed by 19.7% between maxima, located over an opening in the fabric, and minima, located over a knuckle (where two threads of the forming fabric cross). This value decreases to a difference of 4.2% at a distance of 1.5d upstream [53]. From these results it can be deduced that in a hand sheet former, the drainage flow through the paper is more uniform in the XY plane on the top side of the forming paper sheet, and becomes increasingly less uniform towards the wire side.

A certain amount of filler material is free to move with the drainage water. This material has a probabilistic chance of attaching to pulp fibres, or being trapped in the wet web, as it is drained through the thickness of the paper. Thus, regions of the paper that experience a higher flow volume have an increased chance of retaining free filler material. The hypothesis is that the deposition of the filler material that occurs during drainage will not be uniform in the XY plane due to the non uniformities in the flow field. It is expected that areas of the paper formed over an opening in the forming fabric will have a higher concentration of filler material than areas formed over knuckles because of the differences in z-directional flow velocity in these regions. Additionally this anisotropy will be more pronounced on the wire side of the paper than the top side of the paper as the flow becomes less uniform closer to the wire. It is expected that the portions of the sample that experienced flow with the lowest Z-direction velocities will contain less filler, and areas of the sample that experienced the highest

flow will contain more filler. This hypothesis is the focus of the following work – to observe the distribution of the filler material on the surfaces of paper samples in the machine and cross-machine directions.

1.5   Application of SEM and EDX Techniques

Several different imaging techniques have been used in the past to study Z-directional filler and fibre distribution in paper. Some examples include: scanning electron microscopy (SEM) with image analysis techniques, x-ray diffraction (XRD), energy dispersive x-ray analysis (EDX), and x-ray fluorescence (XRF) [48, 55]. These techniques have different advantages when examining different properties of paper and it was found that the coupling of SEM and EDX techniques was the logical choice to quantitatively measure surface filler distribution in paper samples, for several reasons. It has been previously shown that this method allows the user to uniquely study not only the elements present in the sheet but also their quantity and spatial distribution [49]. Using mapping software, the experimenter is then able to create a spatial map, locating the position and concentration of various elements of interest. Finally, the SEM electron beam can be controlled to penetrate only the first few micrometres of the paper surface. This is ideal when only investigating the composition at the surface [49, 56].

The scanning electron microscope is used to image the surface of samples. An image is constructed by firing electrons at a sample. These primary electrons, called the incident beam, are generated by heating a tungsten filament and are accelerated to an energy value between 1 and 30 KeV [57]. The incident electrons strike the surface of the sample and transfer some of their energy to the atoms in the sample. The effect of this interaction is the release of x-rays, backscattered electrons, and secondary electrons. A schematic is shown below.
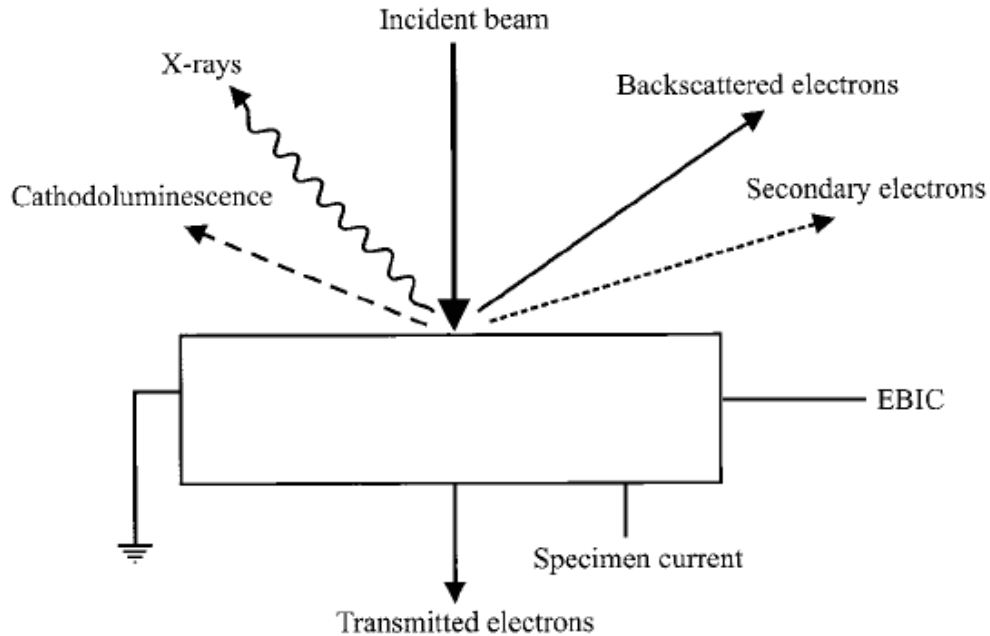
Figure 6: Signals that can be used in the SEM [57]

Secondary electrons are electrons that escape from the sample with an energy below 50 electron Volts. These electrons are generally electrons on the surface of the sample that have received a very small amount of energy from incident electrons and have been able to escape. The yield of these types of electrons can be higher than 1 per primary electrons, and are consequently very abundant. Secondary electrons are the most commonly used signal in the SEM. Backscattered electrons are primary electrons that leave the surface with a large fraction of their incident energy. These electrons are less common than secondary electrons but retain high energies and are used in SEM imaging as well. X-ray and cathodoluminescence beams are generally used in chemical analysis of the sample [57, 58]. The electron beam is focused to a diameter of about 2 – 10 nm. This diameter controls the maximum resolution of the image. The SEM contains sensors which detect backscattered and secondary electrons. The incident beam is moved along the sample surface in a raster scan. The intensity of electrons detected at each location is recorded. An image representing the sample surface is then constructed using the relative intensity of the electron signals at each location [59].

Energy dispersive x-ray spectrometers are used as attachments to the scanning electron microscope to detect the emitted x-rays shown in Figure 6. As electrons from the incident beam bombard the surface of the sample, electrons bound to atoms in the sample can become excited beyond their binding energy and be ejected, leaving an electron hole. If the electron that has been ejected is from an inner shell, the atom is put into an excited state. The atom will eventually relax when an outer shell electron falls down

13

to fill the hole. The difference in energy the electron loses by transferring between the two shells is emitted in one of three ways: a small energy difference is given off as cathodoluminescence, and large energy differences are given off as either a characteristic x-ray or a characteristic electron [60, 61, 57]. EDX detects the presence of the characteristic x-rays. A schematic of the process leading the emissions of a characteristic x-ray is seen below.
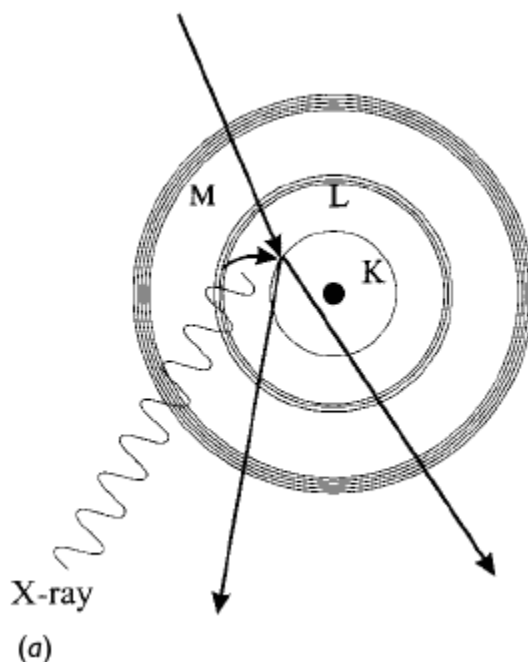
Figure 7: Ejection of K shell electron and the relaxation emitting a characteristic x-ray [57]

The basis of EDX is that the energy and wavelength of a characteristic x-ray is strongly correlated to the atom from which it originated. By measuring the characteristic x-rays and comparing to previously measured values, it is possible to determine which elements are present in the sample [57]. Furthermore, the number of characteristic x-rays detected is representative of the quantity of the element present in the area [57, 58, 62]. The electron beam moves around the sample, focusing on a small area at a time, and the detector tracks the type and quantity of characteristic x-rays it receives. By combining the information at each location, a spatial map of the elemental makeup of the sample is constructed. The resolution of this map is dependent on the size of the incident beam. The nature of this technique meant it was originally only useful in qualitative analysis of samples, but recent technological advances have made quantitative analysis possible as well. EDX has been shown to effectively measure the elemental make up of paper samples in previous experiments [48, 49, 63].

1.6   Research Objectives

It is hypothesised that the variations in the drainage velocity flow field, caused by the geometry of the forming fabric, affect the distribution of the filler material; this idea is the motivation for the following research. The goal was to see how the geometry of the forming fabric affects the surface distribution of the filler material under a variety of papermaking conditions. The surface distribution is of interest because of the implications for printing on a small scale. If the filler material is not evenly distributed, areas of low concentration could become susceptible to misprinting and ink penetration. If the distribution can be better understood, the filler content in the slurry and the forming fabric geometry can be optimised to achieve the desired sheet surface properties.

The main interest was the variation of the filler on a scale of about 1 millimetre – how the concentration changed from one strand to the next in the forming fabric, in both the x and y directions. To conduct repeatable experiments in a controlled environment, the samples were made with the hand sheet former described in chapter 2. The relative concentration of filler material was calculated for areas of the paper formed over different areas of interest in the forming fabric through the use of scanning electron microscope, energy dispersive x-ray spectroscopy, and image analysis techniques. This information was calculated for several different scenarios meant to simulate some of the possible arrangements in a paper machine.

In chapter 3, a plain weave forming fabric was used and other variables were changed. The effects of different filler materials, applied suction (drainage velocity), and presence of retention aids were investigated to see the impact on mineral filler distribution on the paper surface. In most experiments, one variable was changed while the others were held constant. The results represent how the filler concentration varies across a section of paper formed on top of one repeat in the forming fabric.

In chapter 3.4, the surface filler distribution was examined in paper samples made with the single layer, 4-over-1-under forming fabric, X-061088092XCXCB, supplied by AstenJohnson. This experiment was designed to simulate conditions close to those present in an actual paper machine. Chapter 4 covers the conclusions that can be drawn from the results, as well as an outline of the strengths and limitations of the research. Recommendations are made for future work investigating the distribution of particulates in paper.

CHAPTER 2 – APPARATUS AND METHOD

2.1   Experimental Apparatus

The first step in creating laboratory hand sheets is to mix a pulp suspension with the desired properties of the paper that is to be tested. In all cases, the pulp slurry was prepared to 0.5% consistency to simulate the fluid leaving the headbox [6]. Five litre batches were made by mixing the dry material, pulp fibres, and filler into 1.6L of distilled water at 80^oC. This suspension was then mixed at 3000 rpm for 7.5 minutes. Additional distilled water was added to the suspension to bring the consistency to 0.5%. The suspensions were refrigerated when not being used. Before each sample was made, the pulp suspension was brought up to room temperature and continually mixed at 250 rpm. It was previously determined that this preparation method ensures the suspension is uniformly mixed, and represents a sampling error less than 1% [65]. With this method, the suspension tended to flocculate to a moderate degree.

All samples were formed in a custom device meant to simulate a hand sheet former. The apparatus can be seen below in Figure 8. The device consists of an airtight vacuum chamber, constructed of 13mm thick PVC plastic, which acts as the base. This chamber can be opened to the atmosphere or given a negative gauge pressure through the use of the vacuum pump. Extending vertically from the vacuum chamber is a 75 mm diameter, 150 mm tall clear acrylic cylinder which is separated from the base by a fast acting solenoid. At rest, the solenoid is closed and blocks transfer of fluid between the pipe and the vacuum chamber. When triggered, water sitting above the solenoid drains into the vacuum chamber. Above the cylindrical pipe is a horizontal flat plate which supports the forming fabric. The flat plate supports a cylindrical pulp chamber, labelled as the acrylic cylinder in Figure 8. The forming fabric is encircled by a gasket and contained between the flat plate and the pulp chamber. This setup creates an airtight seal when the upper pulp chamber is secured in place, and still allows the forming fabric to be changed between tests.

A pressure transducer, GP:50 Model 218-C-SZ-10-GS, is mounted flush to the pipe wall just below the forming fabric. This transducer measures the pressure drop across the forming fabric, relative to the atmosphere. An ultrasonic distance sensor is mounted above the upper pulp chamber. The sensor measures the height of the pulp suspension as a function of time, the values of which can later be used to calculate the drainage rate of the water through the forming fabric.
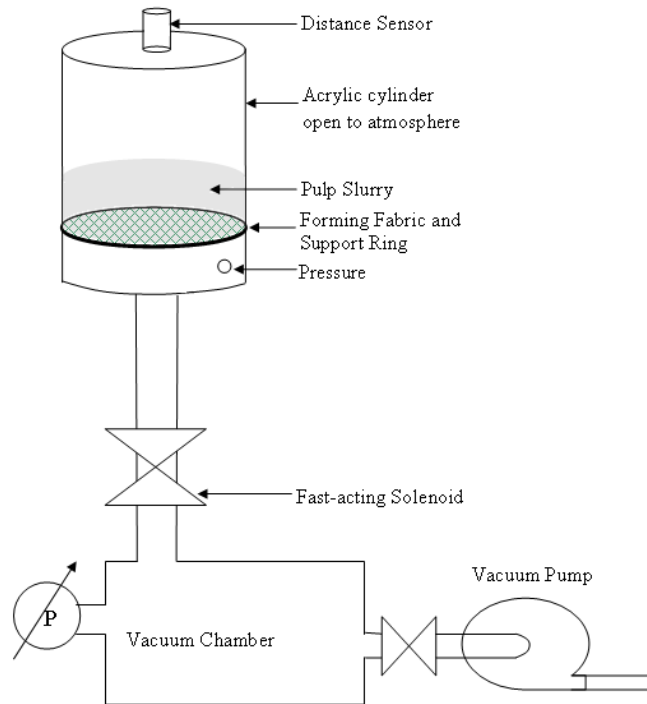
Figure 8: Schematic of laboratory hand sheet former [65]

To make a paper sample, the lower acrylic pipe is filled with distilled water from the closed solenoid to the level of the forming fabric. The desired forming fabric is fitted in place and the upper pulp chamber is attached. A quantity of pulp suspension that corresponds to the desired basis weight of the paper sample, based on the amount of dry material in the suspension, is measured out. If gravity drainage is desired, the vacuum chamber is opened to the atmosphere. If an applied suction is desired, the vacuum pump is activated to bring the pressure in the chamber to the required value. The pulp suspension is then transferred to the top chamber.

A Labview program starts the process by electronically opening the fast acting solenoid, as well as simultaneously starting the recordings of the pressure and distance sensors. With the solenoid valve open, the water from the pulp suspension drains through the forming fabric, and into the vacuum chamber. A fibre mat is formed on top of the forming fabric. The Labview program automatically closes the solenoid after 10 seconds, ending the experiment. The voltage signals from the distance and pressure sensors are put through a low pass filter and saved for further analysis. The samples are then left to air dry on the forming fabric before further processing.

2.2   Controlled Variables in Pulp Suspension

The purpose of this research was to measure the small scale surface distribution of filler material in paper samples, under a variety of conditions. To do this, certain properties of the slurry were varied while others were held constant. The pulp suspensions were made with softwood hydrogen peroxide bleached thermo-mechanical pulp (latency removed, 30% fines) and distilled water to a consistency of 0.5%, to simulate the pulp suspension leaving the headbox in an actual paper machine. All the samples were made at a basis weight of 60 g/m^2.

Two types of filler were used, both at a loading of 40% of the dry mass. A high filler concentration was used in hopes of accentuating the effects of the flow field on the filler distribution. Additionally, as the industry tends towards higher filler concentrations [16], it seemed logical to observe the filler distribution at high concentration values. The first filler type was Albacor HO, a precipitated calcium carbonate (PCC) with the chemical formula $CaCO_3$, which is commonly used in industry. PCC is slightly cationic due to its molecular shape [27]. Since wood fibres are slightly anionic and PCC is slightly cationic, there is an electrostatic attraction between the two. It was hypothesised that this attractive force would resist the effects of the flow field and result in a more uniform filler distribution. To test this theory, Kaolin clay, an anionic, filler was chosen for use in some samples. Kaolin has the chemical formula $Al_2Si_2O_5(OH)_4$ and due to the rough edges of the clay crystals, it is slightly anionic [28]. These two different fillers were used in different experiments to see how electrostatic effects changed the distribution pattern of the filler material under various conditions.

Secondly, the drainage velocity was altered for different experiments. The drainage velocity is directly related to the intensity in the variation of the flow field. It was expected that this would in turn affect the magnitude of filler distribution seen in the samples. At higher drainage velocities, the filler would be more dramatically shifted towards the areas of high flow than it would at lower velocities. Essentially, it was thought that the drainage velocity of the water would be positively correlated to the magnitude of the surface filler spatial variation. To control the drainage velocity with the hand sheet forming apparatus, the applied suction was modified. Two distinct drainage values were used in the experiments. The first was gravity drainage: the vacuum chamber was opened to the atmosphere so that when the solenoid was triggered, the water drained through the forming fabric under its own weight at a velocity of approximately 0.03 metres per second. The second was an applied suction of -10" Hg (-33.86 kPa). Suction boxes in the forming section of paper machines typically range from -15 to -50

kPa [6, 13]. The pressure of -33.86 kPa was chosen because it falls in the middle of the acceptable range, and it was highly repeatable with the pump used in the experiments. This gave an average drainage velocity of approximately 0.12 metres per second.

For each case, both the top and bottom sides of the paper were inspected. The Z-directional drainage flow carried the solid material until it was stopped by the forming fabric. It was expected that on the wire side of the paper, where the paper was being built up directly on the forming fabric, this flow field would be extremely influenced by the geometry of the forming fabric. Consequently, the flow field would be quite varied; as would the distribution of the filler material on the wire side. However, at a distance of the thickness of the paper from the forming fabric, where the top side of the sample is formed, the flow should be almost uniform, which should result in a considerably more uniform filler distribution compared to the wire side. This line of thinking was inspired by the experimental and numerical work done by Peng, Vakil, and others [53, 54, 66]. A numerically determined depiction of the non uniform flow field is shown in Figure 9.
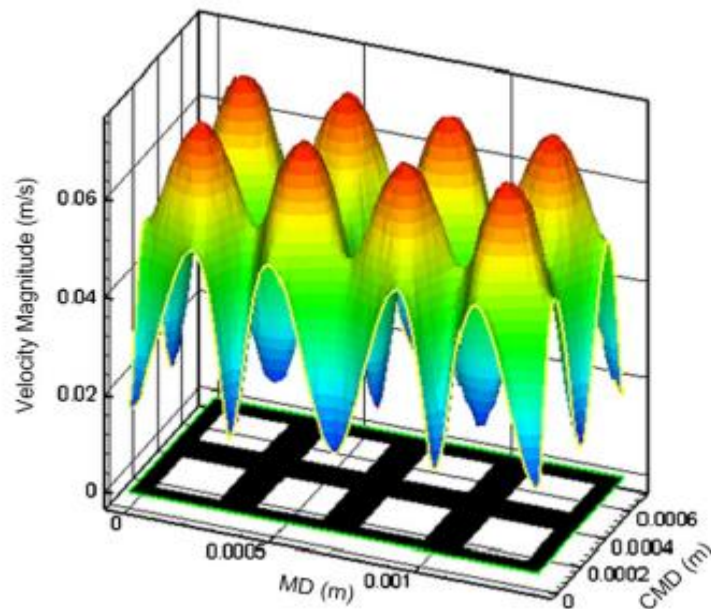
Figure 9: Numerical simulation of flow velocity through a uniform forming fabric [66]

The results in Figure 9 represent the flow in the Z-direction in a plane 0.25d from the surface of the forming fabric, where d is the thickness of a forming fabric thread. It can be seen that at this location, there is a significant difference in the flow velocity. The lowest values occur directly over the area where two threads cross (a knuckle), the velocity over single strands is higher, and the velocity through the openings is highest.

2.3   Method of Data Collection for Plain Weave Experiments

In the first portion of the experiments, a fabric with the simplest weave pattern was used to make the hand sheets. The reasoning for this decision was that if one wanted to see the effect of geometry on filler distribution, it would be considerably more obvious with a simple forming fabric. In a multi-layer fabric, the flow is changed by the location of the strands in each layer, and the interactions between them, but in a single layer fabric, the flow is only modified by the single array of strands. Additionally, the experimental fabric has the most basic weave pattern. Strands are alternately woven above and below each other. This simple grid design is described as "1 over, 1 under" or "plain weave", and can be seen below, in Figure 10. The simple weave pattern means that the size of a repeated element in the fabric is only 2 strands in both the machine and cross machine direction. Thus, every opening experiences the same flow conditions. Essentially, the fabric creates the simplest possible flow field, while still serving its purpose of retaining the large pulp fibres by mechanical entrapment.
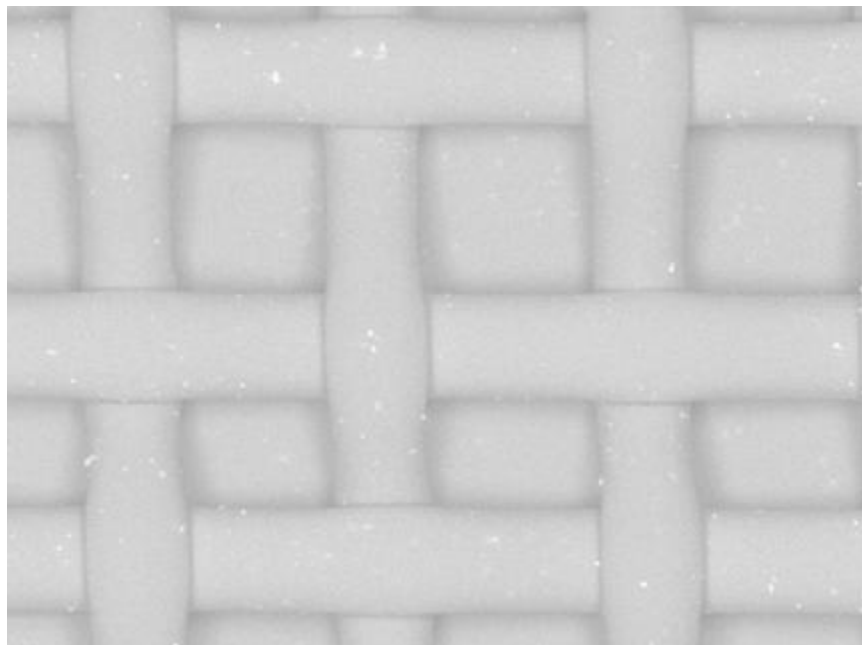
Figure 10: Plain weave forming fabric used in formation of hand sheets

With this design, it is relatively straightforward to correlate sections of a paper sample to the flow field that was responsible for their formation. This becomes increasingly difficult as the complexity of the weave pattern increases, and extremely difficult with multi-layer forming fabrics. This was the primary motivation for the use of this model fabric for the experiments.

It was determined that the local distribution of filler material in paper samples could be determined using Scanning Electron Microscope (SEM) and Energy Dispersive X-Ray Spectroscopy (EDX) techniques. The rationale behind this decision was that if a known area of the paper could be located using the scanning electron microscope, that same area could be analysed with EDX. By tracking elements that are only present in the filler material, a map of the location and density of the filler material could be constructed with the EDX analysis software. With the voltage of the incident beam set to 20 KeV, the electrons penetrate about 10 micrometres into the sample. Thus, when referring to the surface of the sample, the information actually represents 10 microns of depth.

The initial challenge with this approach was locating distinct features of the paper with the SEM. The focus of this work was on the distribution of the filler material at the level of individual strands in the forming fabric. In a broad sense, the interest was in how the filler concentration at the paper surface changes between areas of the paper formed over the unique regions of the forming fabric, which are the threads, the knuckles (where two threads cross) and the openings. To analyse the effect of these regions, the corresponding areas in the paper sample needed to be identified using the SEM – a task that could not be performed by visual inspection. It was decided that the area of paper formed over one full repeat of the forming fabric would constitute a sample. Within a sample, there was paper formed over four different knuckles, four threads, and one opening. To locate the area of the paper formed over one repeat patter, a technique was developed that involved putting pin holes in the paper. The basis of this technique is shown below in Figure 11.
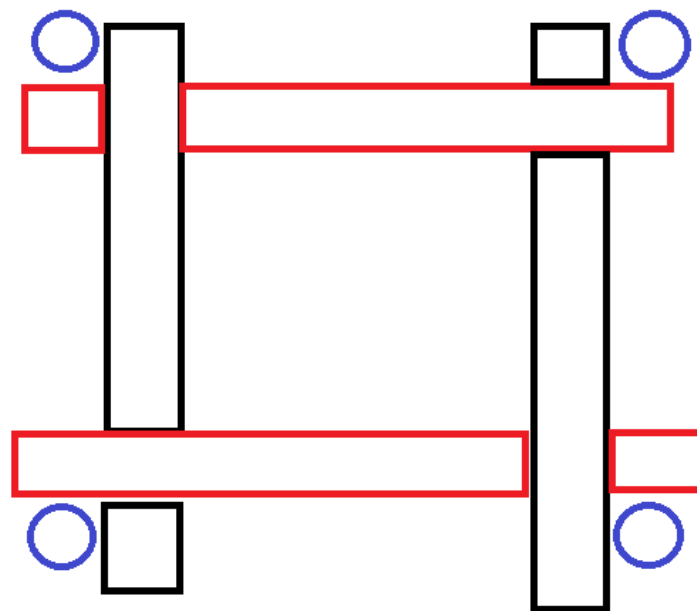
In the above image, the red lines represent the machine-direction filaments of the forming fabric and the black lines are the cross-machine filaments. The blue circles indicate where the pin holes were driven through the paper. To do this, the hand sheets were air dried while still resting on top of the forming fabric. Then, using a microscope and a pin, four holes were created in the paper, just touching the corners of the forming fabric that contained the area of interest. The sample was then detached from the forming fabric and examined with the SEM. The four holes could easily be located with the electron microscope, and it was known that one full sample area was contained within. An example of a SEM image of a prepared sample is shown in Figure 12.
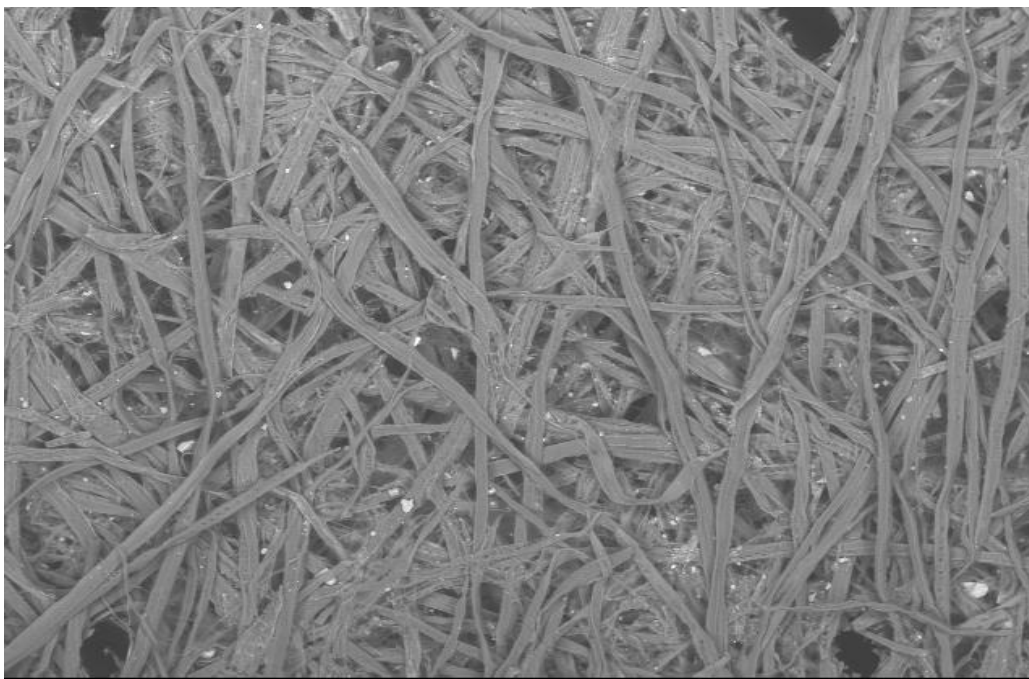
Figure 12: Repeat pattern area is contained within the 4 holes in the sample

The purpose of the SEM is simply to locate the areas of interest in a paper sheet; the spatial information about the filler material comes from the use of EDX techniques. Since the samples were non-conductive, the SEM was operated in low pressure mode, using backscatter electron detection. The image was magnified so that the sample filled the entire field of view of the SEM. The EDX map offered few resolution options; the most detailed of which was 640 x 480 pixels. Therefore, maximizing the magnification reduced the amount of area covered by each pixel, and consequently increased the amount of detail shown by the image. The EDX detector used for these experiments operates with

Quartz Imaging Corporation's XOne X-ray Microanalysis software. The software allows the user to create a spatial map of the atomic makeup of the sample. The mapping function was used in these experiments to plot the location and concentration of filler particles within the paper sample.

This was done by identifying and mapping an element that was only present in the filler material. The paper samples contained wood pulp and traces of water, and thus only Carbon, Hydrogen and Oxygen. The two fillers used were Precipated Calcium Carbonate ($CaCO_3$) and Kaolin Clay ($Al_2Si_2O_5(OH)_4$), in which the unique elements are Calcium, Aluminum, and Silicon. For PCC paper samples, a Calcium map was constructed with the Quartz software and for samples made with Kaolin, the Silicon or Aluminum was mapped. This technique was tested with a control test. A paper sample was made that contained no filler material – only wood pulp. A drop of PCC was then deposited on the dry sample and imaged.

Figure 13: SEM Image of isolated PPC droplet

Figure 13 shows the SEM image of the control test. The left side of the image is the surface of the paper sample made with no filler material. The right side of the image is a portion of the drop of PCC material deposited on the wood fibres. It is clear where the Calcium should be seen in an EDX scan. The sample was then scanned to confirm that the elemental map showed what was expected, the results of which are shown below in Figure 14.
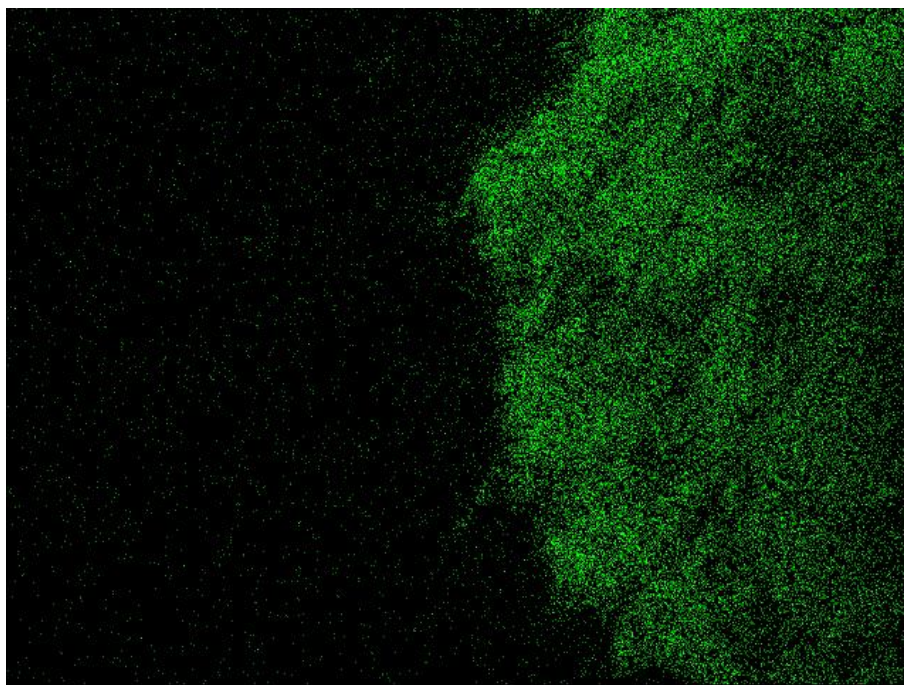
Figure 14: EDX Calcium map of isolated Calcium drop

In this Calcium map, the green pixels represent a pixel where Calcium has been detected. On the left hand side of the image there are a sparse number of green pixels, which is to be expected as the PCC dried and began to migrate slightly. The right side of the image where the PCC drop was located is almost completely covered in green pixels, in the shape of the droplet, as is to be expected. This control test provided initial confirmation that by mapping Calcium, the EDX technique would properly register and represent the presence of Precipitated Calcium Carbonate filler in the paper samples.

A SEM magnification of 60 times was used to analyse the paper samples. This value was chosen because it was the maximum magnification that could be used where all four marking holes fit in the field of view. The mapping images have a resolution of 480 x 640 pixels, so by maximizing the magnification, the amount of area covered by a single pixel was reduced. This increased the spatial accuracy of the elemental map. At 60x magnification, a pixel represents approximately 3.18 μm^2. This is larger than the average diameter of a PCC molecule, which is usually between 1 and 2 μm, so in areas of dense filler concentration, multiple filler molecules would be contained in a pixel area [34]. As can be seen above in Figure 14, the brightness, or intensity, of the green pixels varies. Each time a characteristic Calcium x-ray was received by the EDX detector, the location from which it was ejected (i.e. which pixel) was recorded by the XOne software. These values were recorded for the entire experiment length and used to create the atomic map. If the detector received no Calcium x-rays from a pixel area, it was assigned an intensity

value of zero and shown as black on the map, while the pixels with the highest x-ray count were given the brightest intensity values. The remaining pixels were grouped into bins based on their count number and given a corresponding brightness value.

An atom on the surface of the sample has a probabilistic chance of releasing a characteristic x-ray that will be registered by the EDX detector. A pixel area that contains a high concentration of Calcium is much more likely to release a suitable characteristic x-ray than a pixel area that contains almost no Calcium, since there are more Calcium atoms within the pixel area that are capable of releasing signals. Consequently, in the average sense, areas with higher concentrations of Calcium will release more suitable characteristic x-rays and will be mapped as bright green pixels, while areas with low concentrations will show as dull green pixels [57, 58, 62].

It is important to note that the intensity images shown by the Quartz XOne software (such as Figure 14) do not completely accurately represent the true count values registered by the EDX detector. The figures take the raw count data and divide them into intensity bins, but the intensity bins are slightly skewed in the colour spectrum to make the difference between pixels of different counts more obvious to the human eye. This effect is ideal for visually portraying distribution patterns, but it has the effect of improperly representing the relative concentration when making calculations. To acquire more accurate results, the raw count data for each pixel was extracted from the software and used to calculate relative concentration values. The data is simply a 480x640 array with each entry representing a pixel. The pixel count value represents the number of times a characteristic x-ray was received from the corresponding area of the sample.

2.4 Extraction of Data from EDX Results

After the preliminary experiments, it became apparent that the distribution of the filler was quite chaotic and not easily discernible by examining the elemental map. Figure 15 shows a sample EDX result for precipitated calcium carbonate.
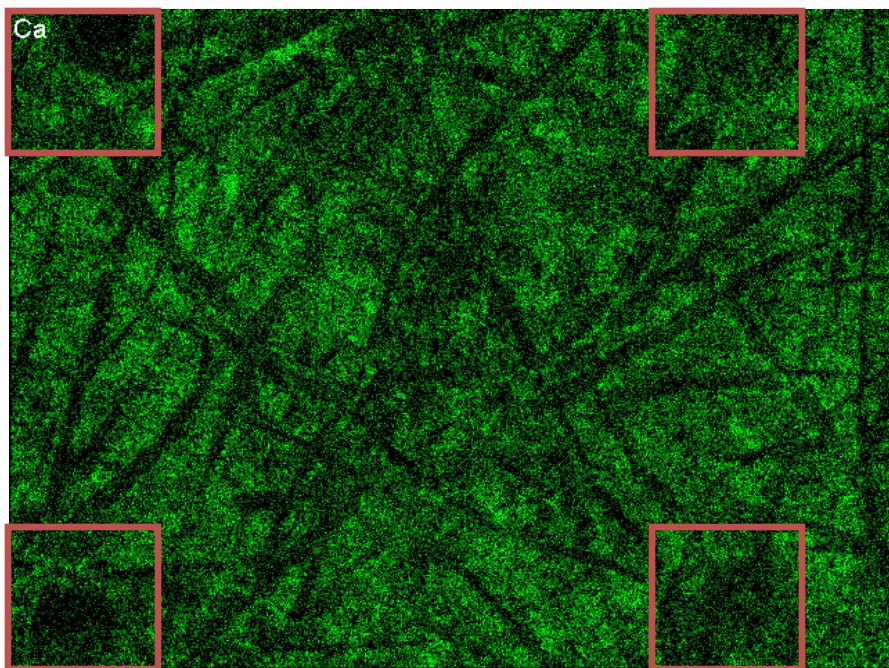
Figure 15: EDX calcium map of repeat pattern of paper

The locations of the 4 holes are highlighted and are quite easy to detect. The effect of the forming fabric geometry, however, is not noticeable to the naked eye. It is not possible to see an obvious variance in the density of green pixels corresponding with the fabric weave. Rather, the location of the pulp fibres plays a significant role in the deposition of the filler molecules. The black streaks in Figure 15 represent the location of surface fibres. It can be seen that filler material tends to collect in the area between fibres. It was thought that the electrostatic attraction of the PCC filler molecules to the wood pulp fibres as well as the physical position of the fibres on the flow field has a very strong influence on the deposition of the filler. As an example, a location where two fibres cross creates a small pocket that tends to retain additional filler material. The effect of the placement of the fibres appears to be so strong that it is masking the distribution effects cause by the non-uniformity of the flow field. Being interested in the distribution caused by the flow field, the effects of fibre placement is viewed as noise. A technique was developed to reduce this noise and allow the underlying flow-related distribution to emerge.

First, it was realised that the filler concentration varies too much from sample to sample (due to the location of fibres) to extract any meaningful information based on individual pixels or even a small area. For this reason, the area of interest, which is contained between the four holes, was divided up into large zones that were expected to have similar properties. Three key areas were identified: the area of

the paper formed over strands of the forming fabric, the area formed over knuckles (where two strands cross) and the area formed over an opening in the forming fabric. By measuring the forming fabric under the SEM, the dimensions of these areas were determined.

Table 1: SEM calculated dimensions of plain weave forming fabric

	Machine Direction	Cross Machine Direction
Thread Centre Line to Centre Line Distance	841 μm	864 μm
Thread Thickness	285 μm	313 μm
Thread Outside to Outside Distance	1126 μm	1177 μm
Opening Size	555 μm	551 μm

Table 1 shows various measurements of the forming fabric from SEM examination. With these values, it was possible to determined which portion of the area contained by the 4 location holes corresponded to paper made over the threads, knuckles, and opening. Using this information, the following zoning pattern was constructed and used in the analysis.

Figure 16: Zoning pattern used for analysis of sample area

As can be seen in the above figure, the paper sample area was divided into four distinct zone types. The four corners labelled K1 – K4 represent the regions of the paper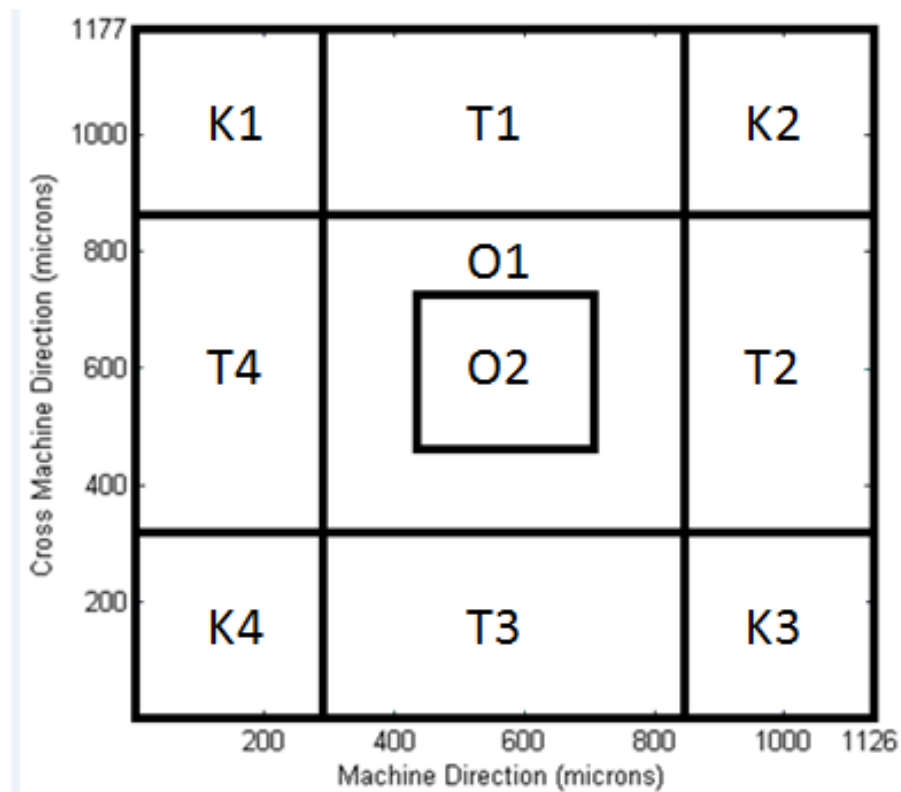 sample formed on the four knuckles of the fabric. T1 – T4 are areas corresponding to the horizontal and vertical threads, and the paper formed over the forming fabric opening is divided into two concentric rectangles, O1 and O2.

The analysis of the EDX maps is a multi-step process to extract information about the filler distribution. First the area of interest was cropped from between the four holes on the EDX image with the image processing toolbox in MATLAB. For the magnification used, this corresponded to a 354x368 pixel image. Each zone represented in Figure 16 was assigned a pixel range, which was calculated from the true dimensions of the forming fabric in Table 1. The true intensity values for each pixel were imported from XOne into MATLAB. Using the pixel ranges calculated from the EDX image, the mean intensity value in each zone was calculate – this represented the average intensity over an area of interest, and consequently the average amount of Calcium, and thus, filler material in that area. This mean value was then normalised with the mean value for the entire sample. This gave a normalised intensity value for each zone in the sample. The purpose of the normalisation was to make the comparison of distribution patterns possible between samples with different total filler concentrations.

The zones were chosen to be such large areas to minimize the noise from the fibre placement. However, this measure alone was not enough to regulate the noise. As an example, if there was a particularly large concentration of filler material in one knuckle due to the fibre arrangement, this gave a completely different picture of the filler distribution than if a similar sample had no filler clumping. To counter this, the normalized results for a sample were averaged on a zone by zone basis between 36 samples. Therefore, to find the distribution of for example, the top side PCC filler distribution under gravity drainage, 36 individual repeat areas were located in the paper and mapped with the EDX software. Each zone was normalised against its sample mean and these normalised zone results were averaged across all the samples. Finally, the values for all similar zones were averaged. The final values for all four knuckles were averaged to obtain a value that was used for all the knuckles in the representation of the results. This was done to effectively quadruple the sample size of the results, and since the forming fabric is the same in all directions, the knuckles all experienced the same flow field and were expected to converge on the same concentration value. Once this significant noise smoothing was completed, a mean distribution of the concentration of the filler material could be seen.

The difference in results between samples is very pronounced. Figure 17 shows the normalised intensity values for the knuckles of the wire side clay experiments. In this case, the water was drained by gravity

drainage, and no retention aids were used. The plot represents the 128 data points collected from the experiments. The knuckle region contained the least amount of filler material in this particular experiment. This meant the mean intensity value in the knuckles was lower than in the threads, outer opening and inner opening. The mean normalised intensity value was 0.944, and is indicated by the horizontal black line in Figure 17. However, it can be seen that the data covers an extremely large range, relative to the mean. The minimum intensity value recorded was 0.643 and the maximum was 1.279. The data has a standard deviation of 0.110, a large spread for a mean of 0.944.
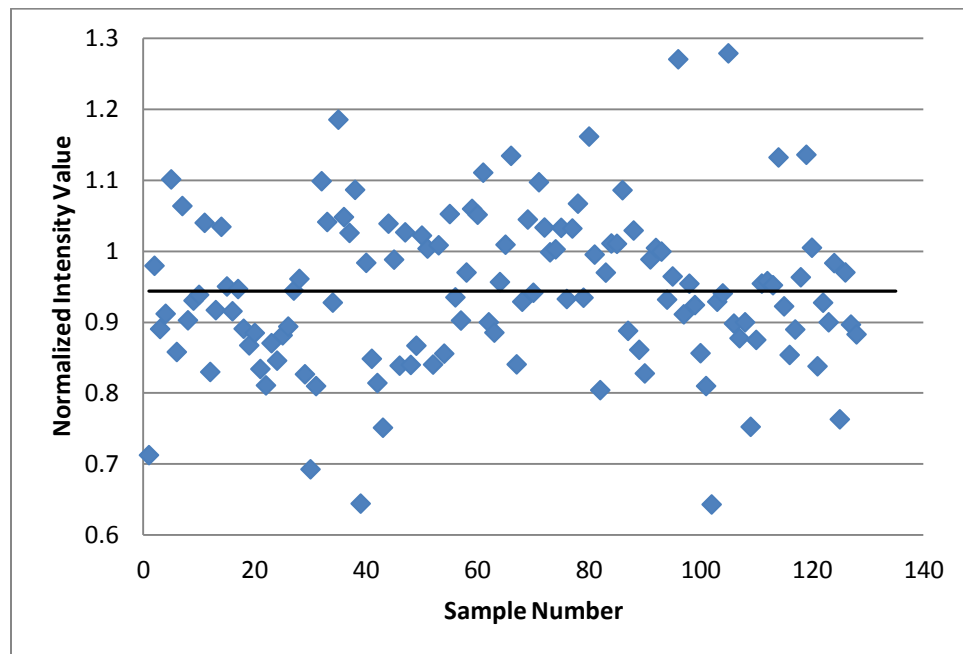
Figure 17: Data distribution for knuckle values from gravity drainage, clay filler experiments

For comparison, Figure 18 shows the 128 data points collected for the outer opening zone of the wire side, clay results with gravity drainage. This was the area containing the second highest amount of filler material, which corresponds to the second largest mean intensity value.
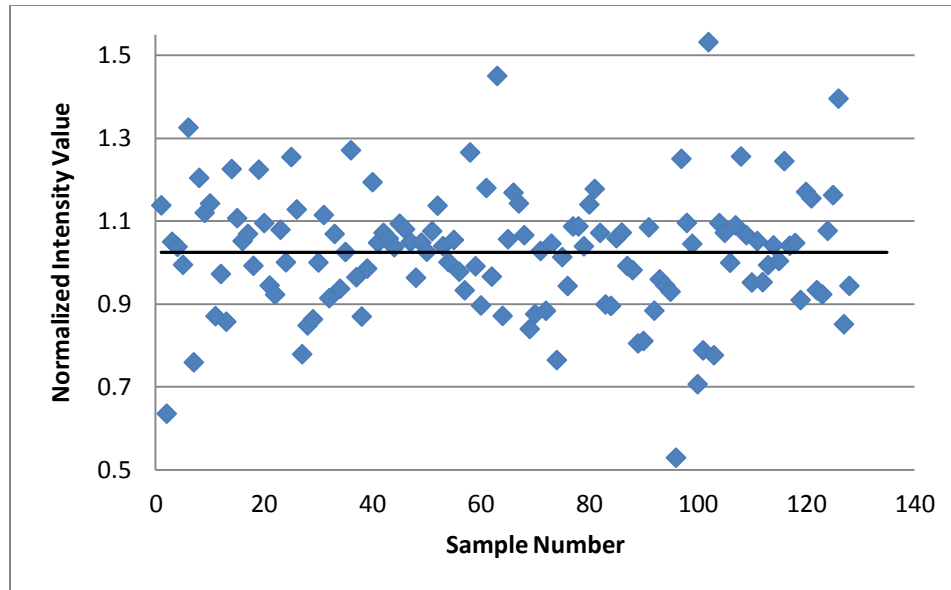
Figure 18: Data distribution for outer opening values from gravity drainage, clay filler experiments

The mean intensity value for the outer opening is 1.025, the minimum value is 0.529 and the maximum value is 1.532. This group of data has a standard deviation of 0.149. Again, the spread of the data is very large compared to the mean value. The standard deviation in this case is larger than that for the knuckle data. The magnitude of the variation of the data justifies the many averaging approaches taken to expose the underlying trend in the spatial distribution of the filler material. The trend is present – it just could not be seen by examining a single sample.

The experiment length is counted in frames; one frame represents a full scan of the sample area. The scan length plays a critical role in the results obtained. Scanning a sample for too few frames will give an inaccurate representation of the location and concentration of the filler material, but the experiments are limited by time, and too many frames would make the investigation of many samples infeasible. An experiment was conducted to determine the ideal scan time for a paper sample. As previously stated, the filler material has a percent chance of releasing a measureable characteristic x-ray during and EDX scan. Thus, the longer the experimental scan time (i.e. the more frames), the more accurate the concentration map produced. A sample was scanned for a varying length: 10 frames, 20 frames, 60 frames, 120 frames, and 360 frames. To determine which scan length should be used for future experiments, the zone values for 10, 20, 60, and 120 frames were compared to the values for 360 frames and the error was computed. This information, in conjunction with the standard deviation of the

data at each frame length, and the time it would take to conduct an experiment were taken into consideration and it was determined that a scan length of 60 frames was optimal. The details of this decision can be seen in Appendix A.

2.5   Evaluation of Industry Forming Fabric

A second forming fabric was used for later experiments. This fabric is made by AstenJohnson and has the reference number X-061088092XCXCB. The intention was to use a forming fabric that is actually used in industry to see how the geometry affects the distribution of the filler material in handsheets. The fabric used in results sections 3.1 to 3.1 has a simple 1-over-1-under geometry which causes a straightforward drainage flow pattern. With more complex fabric geometries, the flow field through the forming fabric becomes increasingly complex and the resulting filler distribution pattern is less intuitive.

The forming fabric X-061088092XCXCB is one of the simplest fabrics used in papermaking. It is made of a single layer "1 over, 4 under" weave pattern. Multilayer forming fabrics can have a very complex effect on the flow field that becomes extremely difficult to model. Thus, the 1-over-4-under style fabric was chosen as a compromise between the two extremes. The design is straightforward enough that it is possible to correlate distribution patterns with a flow field but it is also a fabric that is used in industry with more complexity than the previously used fabric, allowing an understanding of the effects of an industry fabric on filler distribution. The specifications of the fabric are noted in Table 2 and a SEM image at 50x magnification is shown in Figure 19.

Table 2: Specifications of AstenJohnson forming fabric X-061088092XCXCB

Product Name	5-Shaft, Single Layer Monoflex
Number Of Layers	1
Machine Direction Yarn Diameter	0.16 mm
Cross Machine Direction Yarn Diameter	0.19 mm
Paper Side Weave	1, 4 Broken Twill
Air Permeability at 125 Pa – cfm (m^3/s)	570 (0.269)
Fibre Support Index (F.S.I)	146
Drainage Index	54.4
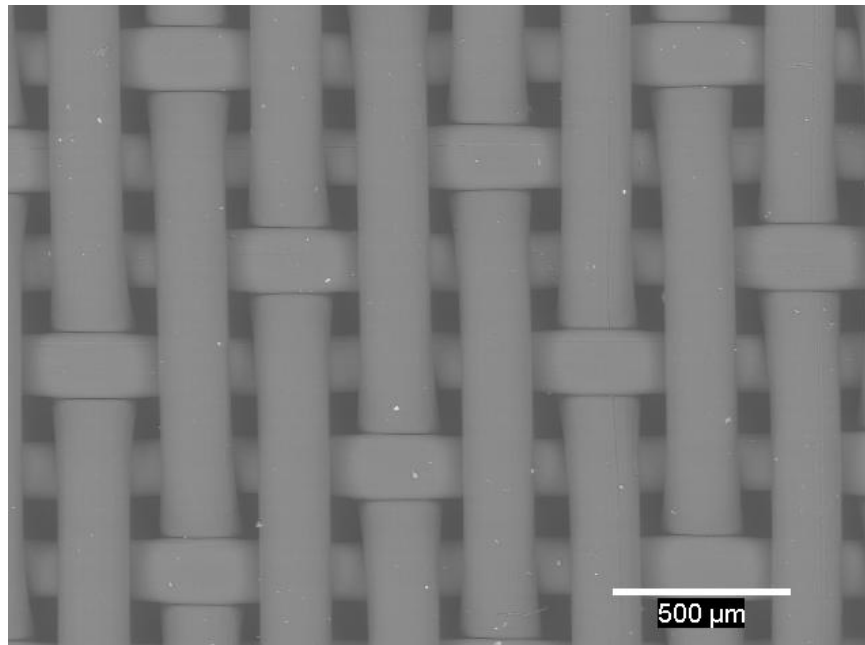
Figure 19: SEM image of forming fabric X-061088092XCXCB at 50x magnification

As shown above, the industry forming fabric, X-061088092XCXCB, is considerably finer than the pressing fabric used in the first set of experiments. It was anticipated that the finer geometry would change the distribution of the filler material to have a more frequent repeat pattern. One of the main goals of industrial forming fabrics is to produce uniform paper. It would therefore be anticipated that the samples produced by this forming fabric would have a more uniformly distributed filler content on the paper surface than those samples produced using the pressing fabric. The goal was to quantify and compare the filler distribution in paper samples made with both fabrics, by examining the normalised filler content in regions of interest.

With this fabric, the procedure of analysis was essentially the same as that described for the samples made on the pressing fabric. Once again, the sample was allowed to dry on the forming fabric, and holes were made in the paper, enclosing one repeat pattern in the forming fabric. The principal difference was that in this case, one repeat pattern constituted a region of 6 threads in both the machine and cross machine direction.
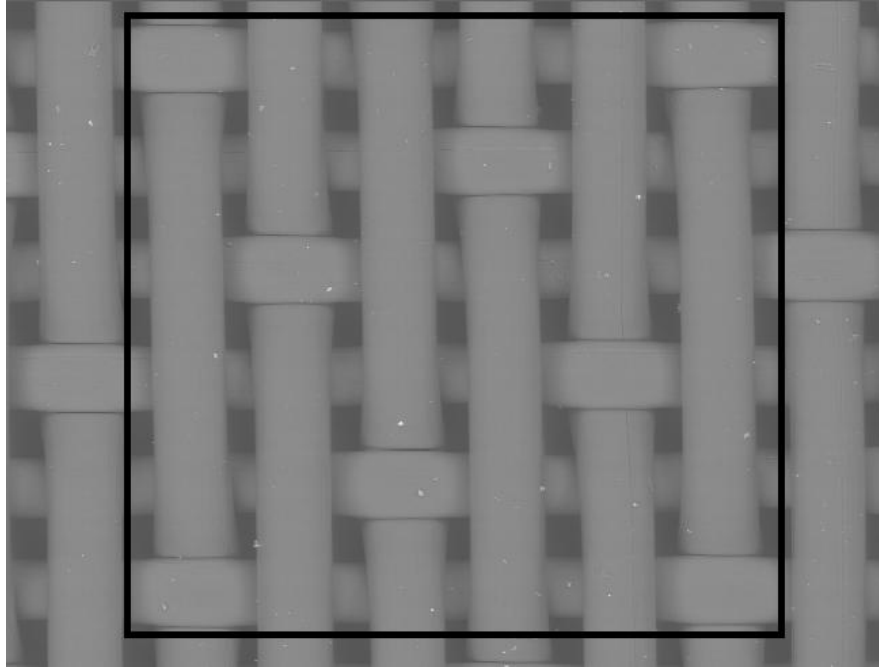
Figure 20: One repeat pattern in the forming fabric

The black rectangle in Figure 20 outlines the area of one repeat pattern in the forming fabric. The largest difference in this case between the two fabrics was that one repeat patter contained many knuckles, openings, and threads and not all like-regions were identical. For example, there were various orientations of the strands surrounding knuckles, which affected the flow field through the region. It was decided that to quantify the filler distribution in paper samples formed with this fabric, it was only necessary to look at the filler content in the areas of the paper formed above the knuckles and the openings since these zones contained the local minimum and maximum filler concentrations, respectively.

The different types of knuckles and threads were classified by the surrounding cross machine directions filaments. Using this method, it was found that there are only two distinct opening regions and three distinct types of knuckles. An outline of this reasoning can be found in Appendix B. Figure 21 shows the two opening and 3 knuckle arrangements present in one repeat pattern of this 4-over-1-under forming fabric.
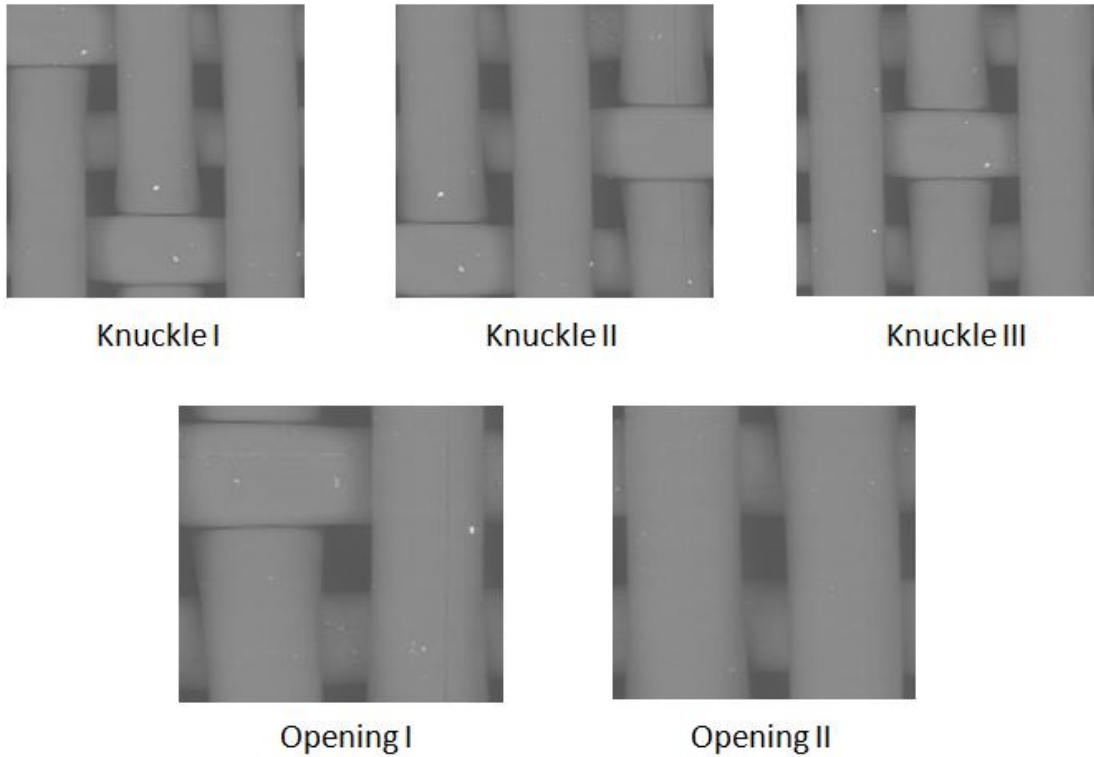
Figure 21: Types of knuckles and openings present in one repeat pattern of fabric

All other openings and knuckles in the fabric were identified as permutations of these five core arrangements. The flow field experienced at any other knuckle or opening would be the same as at one of these five points. With this information, the filler concentration at every knuckle and opening was calculated and used as a data point for the corresponding geometric arrangement. This approach allowed one to acquire a very large amount of data from a modest number of samples.

CHAPTER 3 – RESULTS

3.1 Effects of Filler Type under Gravity Drainage

The experiments of section 3.1 were designed to observe the surface filler distribution in samples made with precipated calcium carbonate and Kaolin clay, in isolation from other formation effects. The vacuum chamber of the apparatus shown in Figure 8 can be opened to the atmosphere or sealed off. When open to the atmosphere, the water is drained from the pulp suspension purely by the force of gravity. The following results are conducted on samples formed by gravity drainage with no retention aids.

Figure 22 shows the wire side results for a sample made with Precipitated Calcium Carbonate filler at a concentration of 40% of the dry mass, under gravity drainage. The areas representing the paper formed over top of the knuckles of the forming fabric have the lowest filler concentration of all the zones. These areas are below the average level for the whole sample by 1.5 percent. The areas of the paper formed over threads do not differ from the mean sample filler concentration level. Conversely, the outer square of the interior region, which corresponds to the outer area of the paper formed on top of an opening in the forming fabric, is above the mean filler concentration by 1.9%, while the innermost area has 3.7% more PCC than the mean. These values were found to be statistically significant, through the use of Student's t-test on a confidence level of 95%. See Appendix C for sample t-test calculation.

This initial result was extremely important because it confirmed the hypothesis that the areas of the paper that corresponded to formation areas of greater flow velocities would have a higher concentration of filler material. As the water is drained through the forming fabric, the flow velocity will be greatest in the centre of the opening, less at the sides, less still over the threads and lowest of all over the knuckles [53, 54]. The original hypothesis did not cover the magnitude of this effect, though it was reasoned that a range of variables would affect the filler distribution. In the case of the PCC filler distribution on the wire side of samples formed by gravity drainage, it was found the maximum difference in filler concentration occurred between the paper regions formed over the knuckles and the inner opening. This value was calculated to be 5.2%. The maximum difference is used often in the following results to quantify the severity of the anisotropy of the filler.
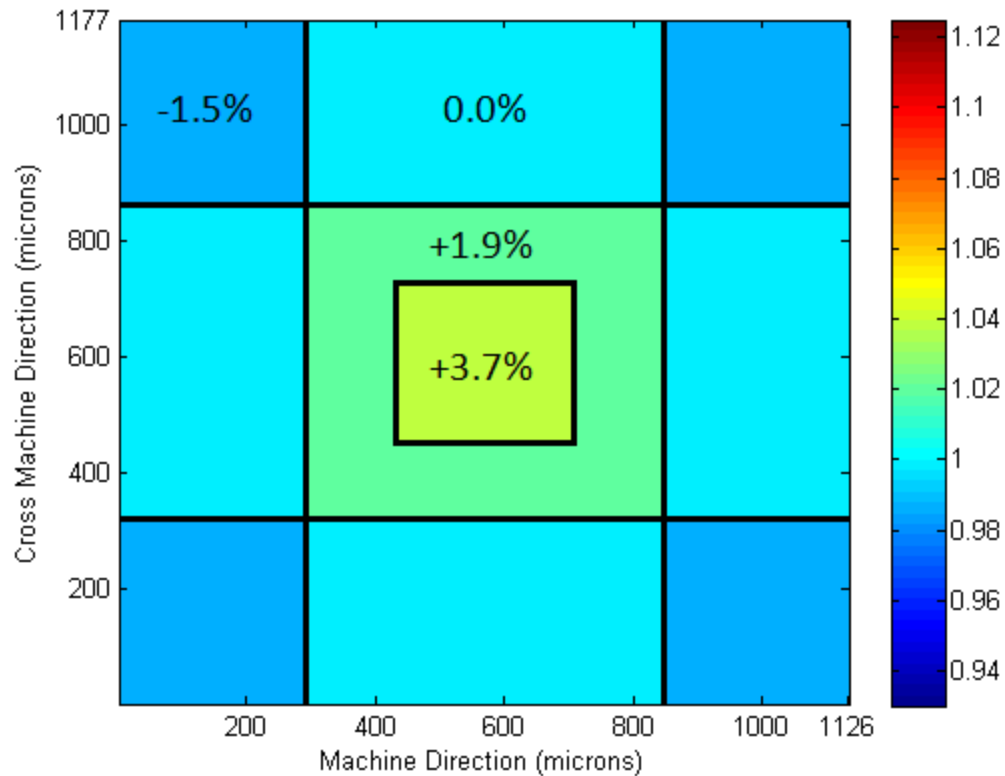
Figure 22: PCC filler distribution for wire side gravity drainage

Following the wire side, the top side of samples formed under the same conditions was investigated. Once again, the area of the paper that was formed over knuckles in the forming fabric showed the lowest concentration of filler material. In this case, the concentration was below the sample mean by 0.5 percent. The thread area was very close to the mean, having 0.1 % more filler, while the outer opening area was found to contain +0.5% and the centre +0.8%.
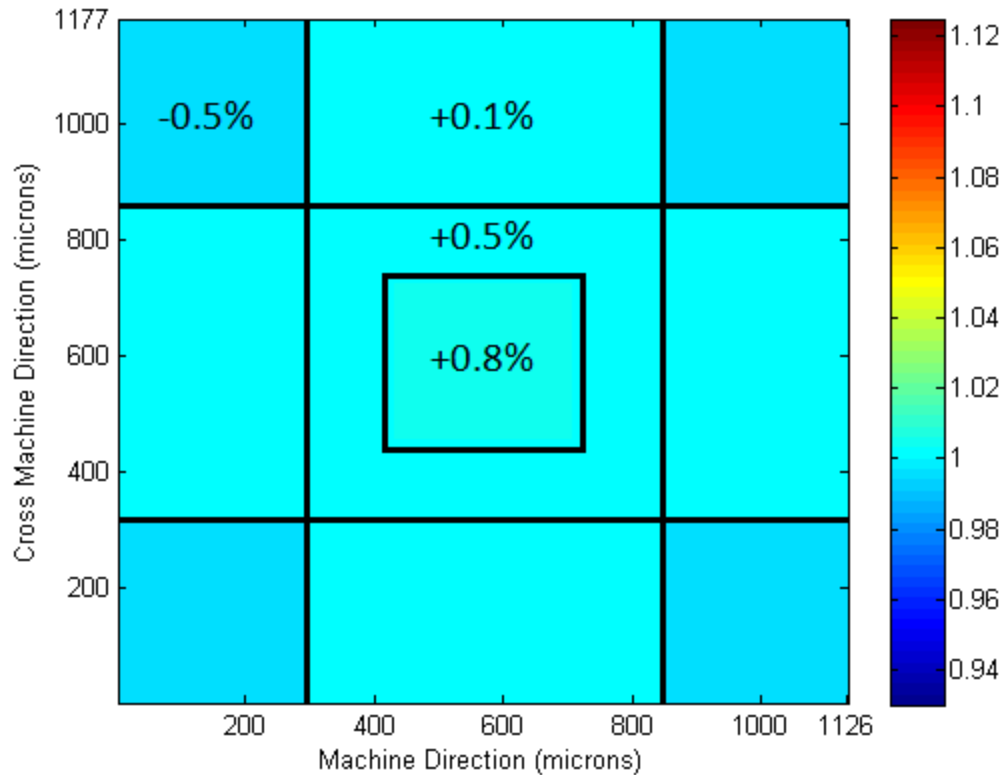
Figure 23: PCC filler distribution for top side gravity drainage

These results further support the initial hypothesis. For the top side of the paper, the distribution of the filler material shows the same general trend as the wire side results, but the magnitude of the variation is significantly reduced. This makes logical sense when the flow field is considered. The geometry of the forming fabric will have a very strong effect on the drainage flow on the wire side of the paper. At a distance of the thickness of the paper from the forming fabric, the fabric has a smaller effect on the flow, resulting in a more uniform flow field. This flow field is what directs the deposition of the material that ends up forming the topmost side of the paper. Consequently, the distribution of the filler material is more uniformly distributed on the top side than the wire side, though the effect of the flow field is still present.

Wood pulp fibres are slightly negatively charged and precipitated calcium carbonate is slightly positively charged, in distilled water [23, 27]. This combination results in a slight electrostatic attraction between the PCC filler material and the wood fibres. This force would tend to resist the force of the flow field as the filler material clings to the wood pulp. To test this reasoning, by further accentuating the effects of the flow field on the distribution, samples were made with Kaolin clay ($Al_2Si_2O_5(OH)_4$) instead of PCC. Kaolin is slightly negatively charged so rather than being attracted to the wood pulp fibres, it should

experience minute repulsion [28]. It was hypothesized that this would result in a more pronounced distribution in the filler material than when PCC is used.

Similar to the PCC case, the experiments were repeated on the top and bottom sides of the clay filler paper. Gravity drainage was used and the filler made up 40% of the dry materials, by weight. The results are shown below, in Figure 24.
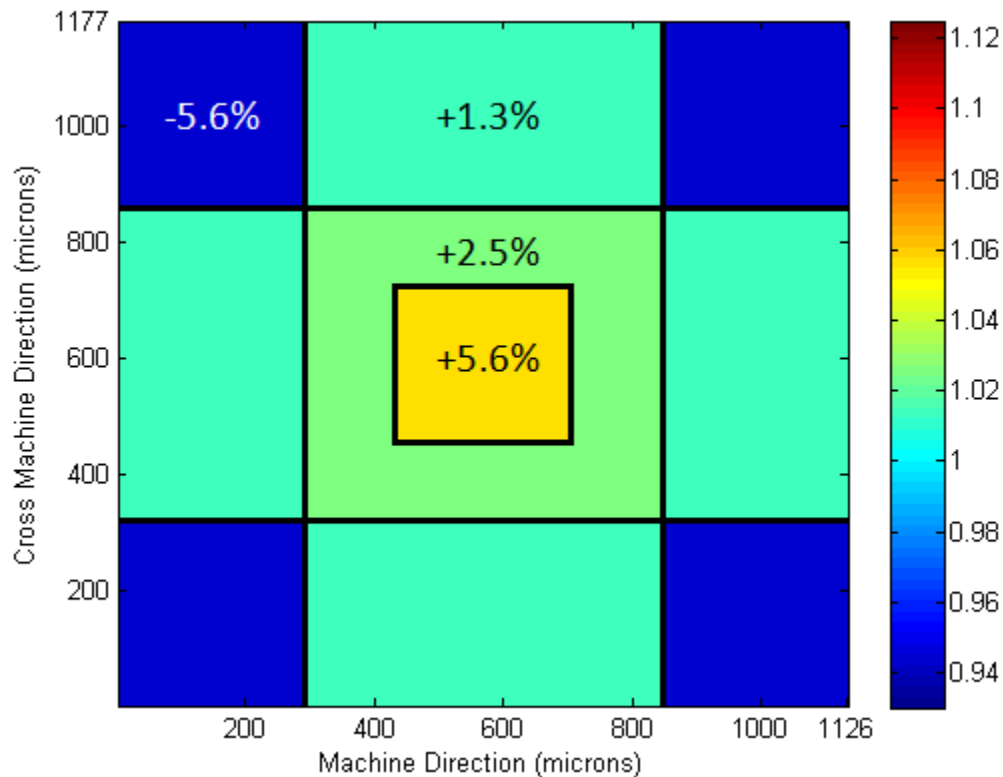
Figure 24: Clay filler distribution for wire side gravity drainage

Once more, we see that the general trend of filler distribution is present. The most important point to observe with these results is the significant increase in variation between the opening and the knuckles relative to the wire side precipated calcium carbonate case. Both samples experienced the exact same dewatering conditions, caused by gravity drainage. Thus it can be seen that the filler type has a large impact on the filler distribution on the paper wire side surface. The discrepancy between the two results is believed to be caused by the slight attractive electrostatic force between the PCC and the wood pulp fibres and the slight repulsive force experienced by the clay. It is also possible that some of the discrepancy is due to the difference in filler particle geometry. The shape of PCC particles is generally uniform and consistent, while Kaolin is more random and fragmented. The uniform shape could aid in uniform deposition, as all particles will experience similar effects from the flow field.

The difference in concentration between the knuckles and the inner area of the opening is approximately 11.2%, over double that exhibited with PCC filler. Significantly more filler has been moved from the knuckles to both the thread and the opening regions. It was hypothesised that the distribution would be more pronounced with clay filler, but the magnitude of the discrepancy was not anticipated. It is apparent that under these formation conditions, the electrostatic attraction between PCC filler and wood pulp is quite strong.

Again, the experimentation and analysis was repeated on the top side of the clay filler paper. The result is shown below in Figure 25.
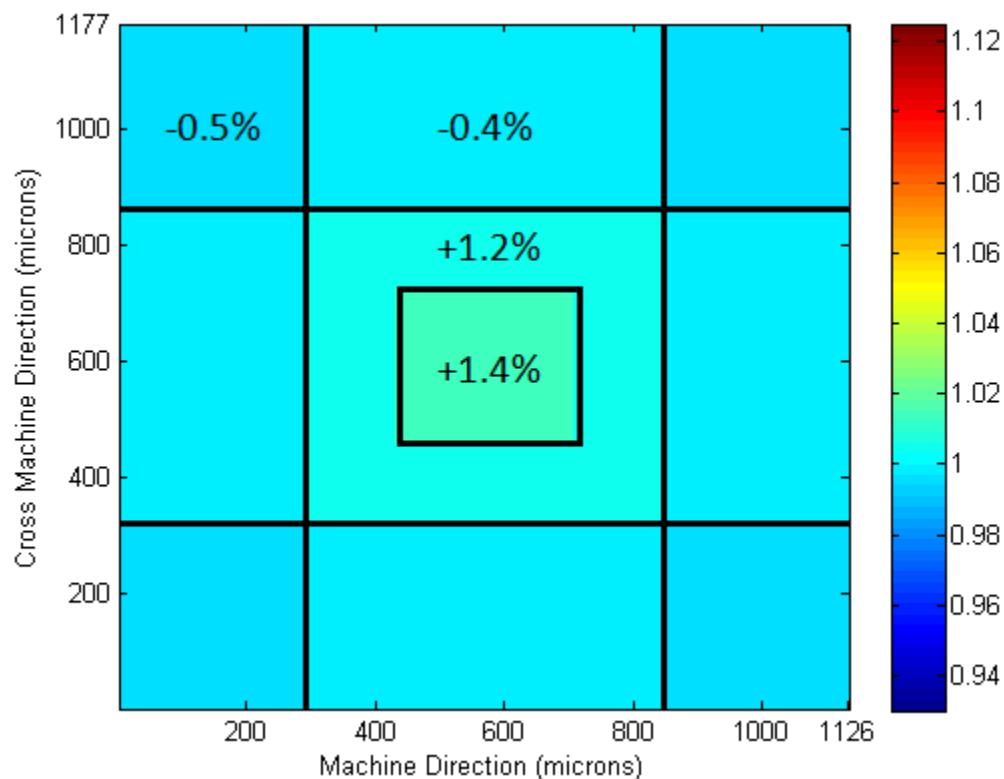
Figure 25: Clay filler distribution for top side gravity drainage

As seen in Figures 22 and 24, the variance of the distribution of the clay filler on the wire side of the paper was over twice as extreme as the distribution of the precipated calcium carbonate filler on the wire side. It was expected that when comparing the top side results of the two cases, the ratio between the distributions would be comparable to the ratio on the wire side. This means that, having seen a maximum difference of 1.3% on the top side of the PCC sample, it was expected to detect a variation in the range of 2.8% for the top side of the clay sample.

However, it was found that the maximum clay distribution on the top side was 1.9%. This difference in the filler distribution ratio between filler types on the two sides is once again cause by the variability of the flow field in the Z-direction from the forming fabric. During the formation of the top side of the samples, the forces redistributing the filler material are not very strong. Consequently the clay material is concentrated in areas of high flow to a greater degree than the PCC (due to the electrostatic bonding), but this effect is relatively small compared to the discrepancies on the wire side.

3.2   Effects of Vacuum Drainage

In this section, the effect of the dewatering rate on the surface distribution of filler material is examined. The results from the previous section, where the water removal was due to gravity drainage, represent sets of data for one dewatering rate. For comparison, the same 4 cases - top and wire sides of paper with precipitated calcium carbonate and kaolin clay filler - were reproduced using vacuum drainage. All other specifications were held constant for these experiments. The forming fabric, suspension consistency, filler percentage of dry mass, and sheet basis weight are the same as for the experiments in section 3.1.

The suction used for dewatering was -33.86 kPa. It was expected that the higher drainage velocity associated with suction dewatering would cause a more dramatically varied flow field. This in turn should cause the distribution of the filler material to be more pronounced than in the corresponding gravity drainage case. It was anticipated that the effect of the different filler types would continue to play an effect. That is, the samples containing clay filler would show a more dramatic variation between the knuckles, threads and opening regions than the samples made with PCC. However, the magnitude of this effect was unknown and not predicted, and it was unclear whether the increased drainage velocity would tend to enhance or diminish the distribution discrepancies between the two types of filler material.

The first case with vacuum drainage was the wire side of the paper containing clay filler. These results are shown below in Figure 26. This distribution is characterized by a maximum variation in the filler concentration of 16.4% between the knuckles and inner opening. This value is approximately 46% greater than the 11.2% difference between the knuckles and inner opening for the gravity drainage case. Thus, for clay filler material, an increase in applied suction from gravity drainage to 33.86 kPa

causes a 46% increase in the variation of the filler material. It is also interesting to note that the relative concentration in the knuckles is very similar for both the gravity and vacuum drainage cases. The area of the paper formed over top of the threads of the forming fabric contains less filler material in the case of vacuum drainage than gravity drainage. The gravity drainage result contains a higher filler concentration in the thread regions. The augmented velocity of vacuum drainage relocated filler material from the threads to the opening zones of the paper.
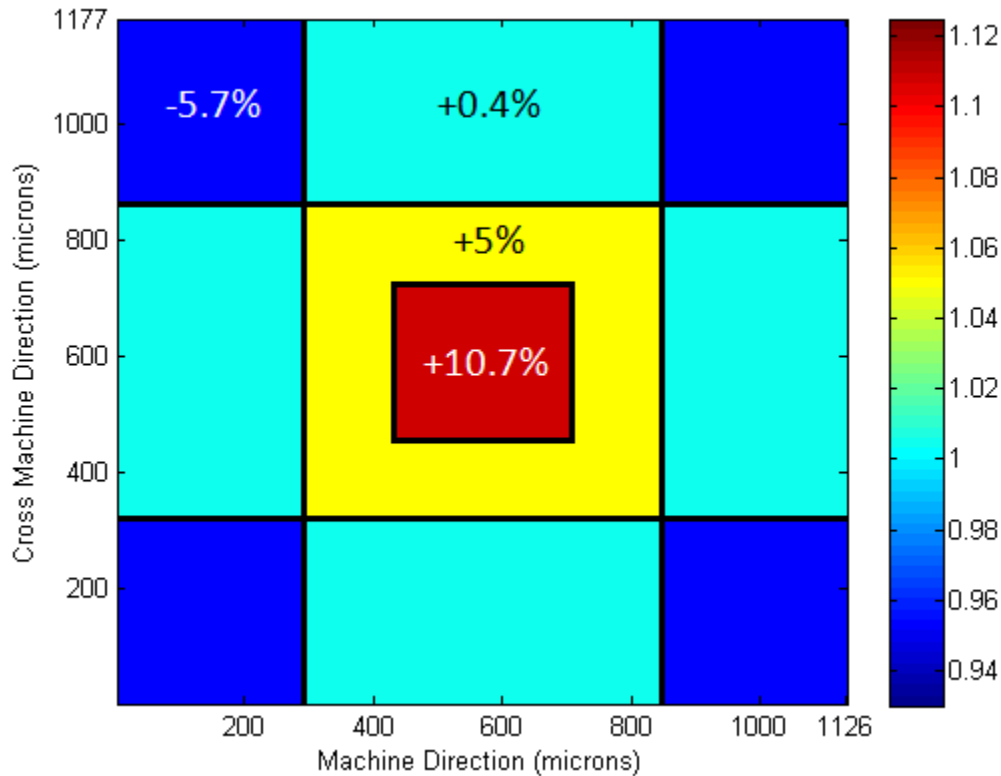
Figure 26: Clay filler distribution for wire side vacuum drainage

Next, the top side concentrations of the clay filler samples under gravity drainage were computed. The thermal map of this result can be seen below, in Figure 27. Once more, the distribution on the top side of the sample is quite uniform. The maximum difference in concentrations, occurring between the knuckles and inner opening, is 2.0%. This value is essentially identical to the concentration spread found for the top side of the PPC paper and clay paper produced under gravity drainage.

This is an intriguing result; it seems as if the dewatering velocity has a limited effect on the distribution of the filler material on the top side of the paper. As previously discussed, the uniformity of the flow field quickly increases with distance upstream of the forming fabric, causing the formation of the top side of samples to be governed by a relatively uniform flow. It is thought that although the wire side

velocity gradients are much larger under vacuum drainage than gravity drainage, on the top level, the flows are comparable between the two cases. And since the flow fields are quite similar, the resulting top side distribution patterns will also be similar. A minor difference in the flow field likely results in only a slight change in the distribution pattern. This explains the similarity between the top side vacuum and clay results.
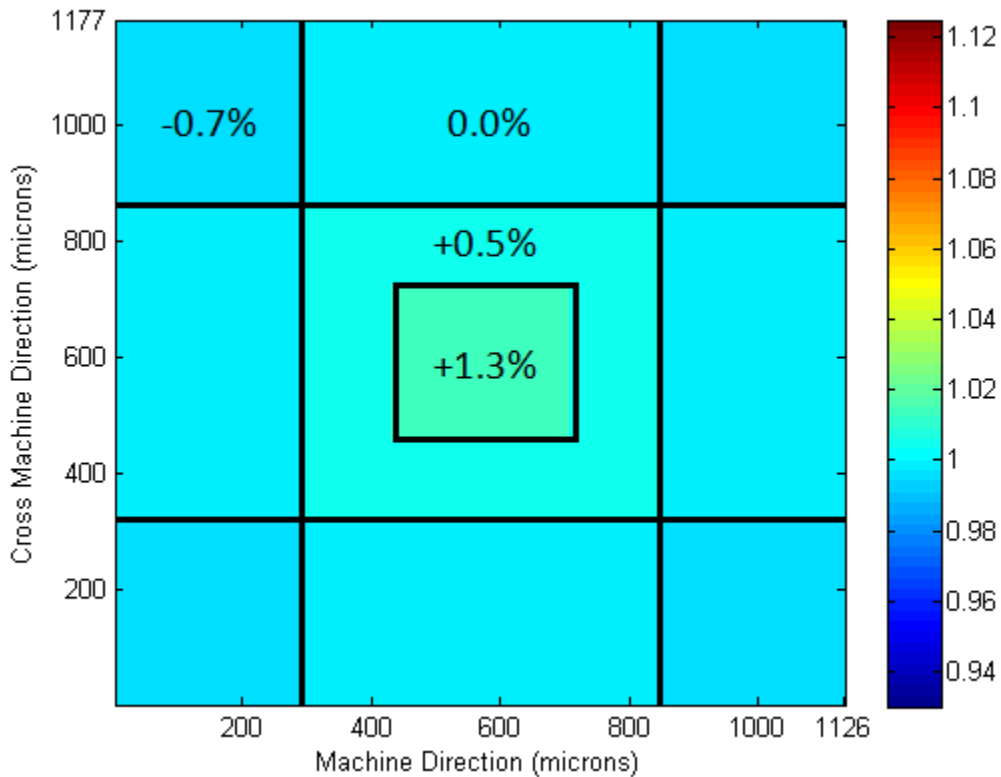
Figure 27: Clay filler distribution for top side vacuum drainage

Similarly, the process of determining the local filler distribution on the top and wire side of the paper was repeated with PPC samples. The results for the wire side are shown in Figure 28. This finding is of particular note because for all the cases studied, it contains the lowest concentration of filler material in the sample area formed on top of the knuckles, and the most in the area corresponding to the threads. The opening still contains the most filler material of the zones, and the knuckles the least, but the magnitude of these differences is unique.
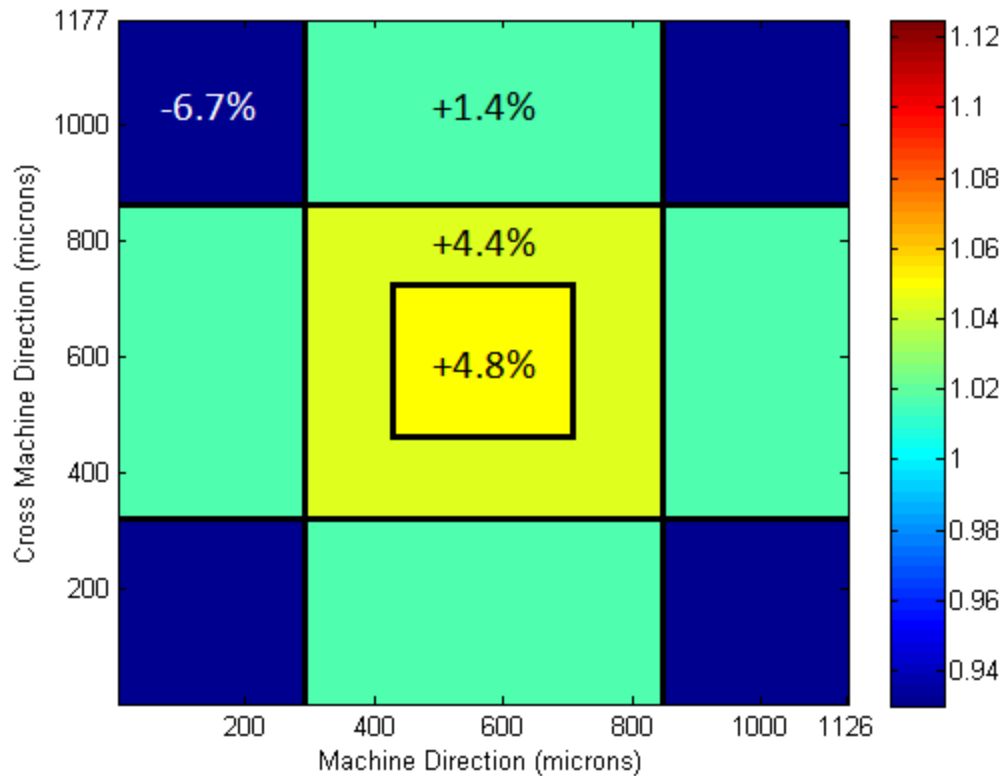
Figure 28: PPC filler distribution for wire side vacuum drainage

In the case of the PPC sample under gravity drainage, the knuckles contained 1.5 percent less filler than the mean value, and the inner opening contained 3.7 percent more. In this case, with vacuum drainage, the knuckles are below the mean by 6.7 percent and the inner opening is above by 4.8 percent. It was expected that the ratio between the knuckle and the opening concentrations seen in the gravity case would be observed again in the vacuum case, but exaggerated by the higher intensity flow field. This was obviously not the case, as the percentage removed from the knuckles more than quadrupled, while the percentage added to the opening increased by about 30%. The maximum filler variation, which is calculated as the concentration difference between the knuckles and the inner opening, is 11.5%, which represents a 121% increase in the maximum difference from the gravity drainage case.

The peculiarities of this change are compounded when compared to the results for the clay samples. Comparing the gravity drainage and the vacuum drainage results for clay, the maximum difference between the knuckles and opening increased by 46%. From this we conclude that a variation in drainage velocity has different effects on pulp suspensions made with different fillers. This is attributed to the nature of the electrostatic bonds formed between PCC filler and wood pulp fibres. The bonds are susceptible to being broken by larger shear forces, so under gravity drainage where the shear is low, the

bonds tend to hold and the filler material resists the distributing effect of the flow field. However, under vacuum drainage where the shear forces are higher, more electrostatic bonds are broken and the filler material distribution follows the flow field more closely. Consequently, the distribution difference between the clay and PCC fillers is minimised. Thus, distribution of filler that is electro-statically attracted to the wood pulp fibres will be significantly more affected by an increase in applied suction than filler that is repelled by the fibres.

Finally, the distribution was calculated for the top side of the PCC filler samples. It can be seen in Figure 29 that the areas of the samples formed over knuckles contain 0.8% less filler material than the sample mean. The sample area corresponding to the threads of the forming fabric contains 0.2% more than the mean, the outer opening represents an increase of 0.5% and the inner opening has 0.7% more filler material than the average for the entire sample. The maximum difference occurs between the knuckles and the inner opening, and this value is equal to 1.5%. This is an interesting result in comparison with the top side PCC samples under gravity drainage, where the maximum difference (also between the knuckles and inner opening) is 1.3%.

As mentioned above, the effect of the applied vacuum increased the maximum difference between zones by 121% for the PCC wire side results. On the top side, this change is only 15.4% between the two cases. This result reaffirms that although the more dramatically varied flow field caused by vacuum drainage has a significant effect on the filler distribution on the wire side of the paper, the variance quickly diminishes with distance from the forming fabric. Thus the flow field at the level of the top side of the paper is comparable between the cases of gravity and vacuum drainage. Consequently, the top side filler distribution pattern is comparable for gravity and vacuum drainage. This same effect was observed with the clay filler samples, as well.
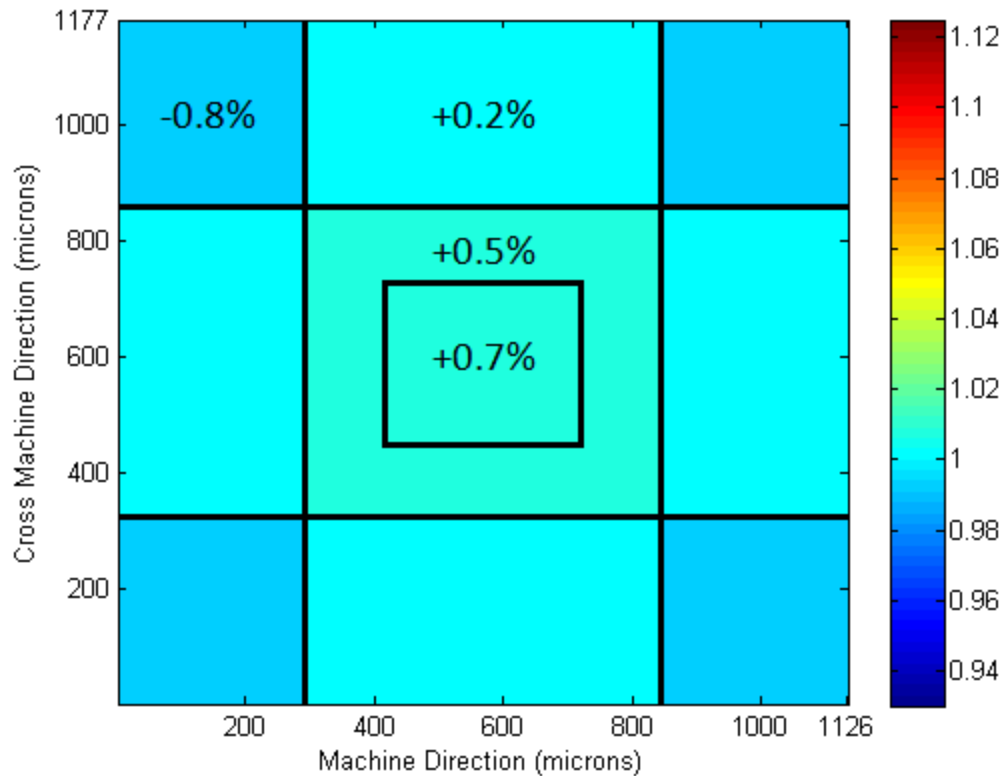
Figure 29: PPC filler distribution for top side vacuum drainage

This section highlighted the differences in filler distribution caused by formation suction pressures. In general, a greater applied suction was shown to increase the filler distribution on the paper surface by intensifying the variation in the local flow field over the knuckles, threads, and openings of the forming fabric. Under gravity drainage, the wire side clay results are considerably more varied than the PCC wire side results, an effect that is attributed to the electrostatic attraction between the cationic PCC particles and the anionic pulp suspension. However, under vacuum drainage, the maximum difference in the zones increased significantly more for the PCC filler wire side results than the clay. This result is attributed to the susceptibility of the electrostatic bonds to high shear forces. With a greater drainage rate due to the applied suction in vacuum drainage, the attraction of the filler to the wood fibres is largely overpowered by the force of the drainage water – essentially minimizing the distribution gap between the PCC and clay distribution. Furthermore, it was found that the increased flow field variation caused by higher drainage rates dropped off dramatically as distance from the forming fabric is increased. Consequently, for both the clay and PCC cases, on the top side of the paper, the filler variation increased only marginally with an increased dewatering rate.

3.3   Effects of Retention Aids

Another area of interest was the effect on the filler distribution of adding retention aids to the pulp suspension. As explained in section 1.3, retention aids work to retain more filler and fine particles in the final sheet of paper through charge modification and macromolecular bridging. Essentially, the retention aids help bind the micro particles to each other and to the larger wood fibres, keeping the small particles from being drained from the wet web of the paper during the dewatering process. With this in mind, it was hypothesised that paper containing retention aids should not only have a higher concentration of filler material than the corresponding samples without retention aids, but the distribution of this filler material should be more uniform when retention aids are present. It is thought that the bonds that hold the filler material to the fibres will act in a similar manner to the electrostatic attraction between PCC filler and pulp fibres. That is, to reduce the variation of filler concentration by preventing the filler from moving freely with the flow field.

To investigate the effect of retention aids on filler distribution, the specifications of the hand sheet former were set to simulate industry forming conditions. Thus, the top and wire side of paper samples with PCC filler and retention aids, under the effect of vacuum drainage, was investigated. As a comparison, a third experiment was conducted on a sample made from the same slurry, using gravity drainage. Initially the overall concentration of the PCC filler material on the wire side of the sample was tested to verify that the retention aids were performing as expected.
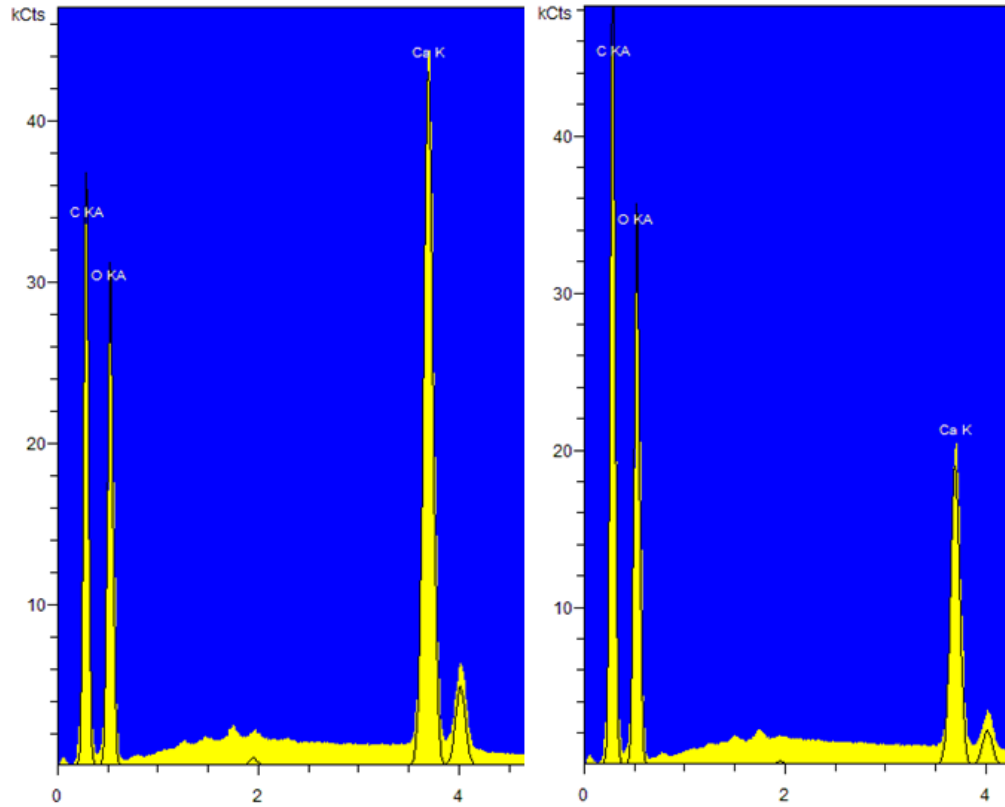
Figure 30: Quantity of elements present in wire side PCC samples with retention aids (left) and quantity of elements present in wire side PCC sample without retention aids (right)

The spectra in Figure 30 show the results from EDX scans of paper samples with (left) and without (right) retention aids. The peaks represent a count of the number of characteristic x-ray detected by the device for each element. Thus, the considerably larger Calcium peak in the left image indicates that there is much more filler material present on the wire side surface of the samples when retention aids are used.

The first result, presented in Figure 31, shows the distribution of PCC filler on the paper wire side, under the effect of vacuum drainage, with retention aids used in the suspension. It can be seen that the knuckles contain 6.5% less filler material than the sample mean, the threads contain 1.7% more, the outer opening region's PCC content is 4.4% above the sample mean, and the inner opening zone has the highest filler concentration with 4.8% more PCC than the sample average.
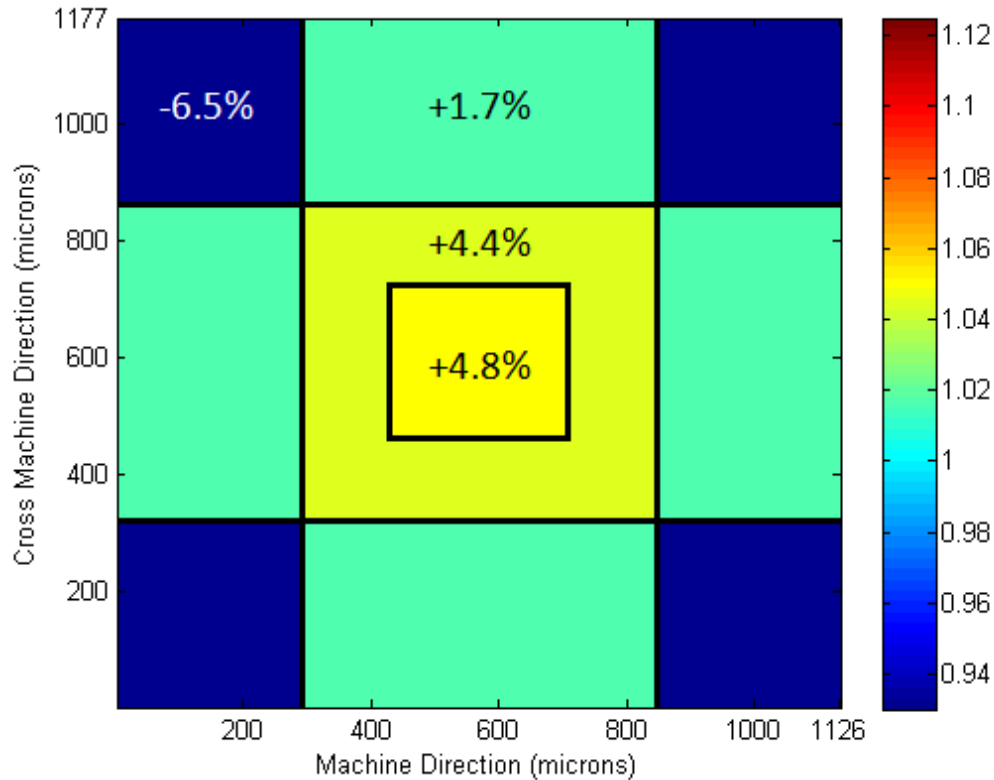
Figure 31: Wire side PCC filler distribution under vacuum drainage with retention aids

This result was very interesting, considering the results for the same experiment without retention aids: there is almost no difference in the maximum distribution. With the presence of retention aids, the maximum difference between knuckle and opening is 11.3%, and without retention aids, the same parameters yielded a difference of 11.5%. Having expected the retention aids to make the sample filler distribution more uniform, this result was unanticipated. A possible explanation for this phenomenon is that the flocs formed by retention aids are susceptible to being broken by large hydrodynamic shear forces [35, 40]. Essentially, the same effect is occurring that explains the similarities in clay and PCC filler distribution with vacuum drainage. In cases where the water is drained from the sample rapidly, such as when a large applied vacuum is used, the shear forces of the water acting on the filler material are very large. The forces overcome the bonds between the filler and fibres, and strip the filler material from the fibres. Consequently, on the wire side of the sample under vacuum drainage, where the flow is quickest, the effects of the retention aids are overpowered by the flow field. The resulting distribution pattern is essentially the same, whether or not retention aids are present in the pulp suspension.

The effects of retention aids on the PCC filler distribution under vacuum drainage was also observed on the top side of the paper. These results are shown in Figure 32.

48
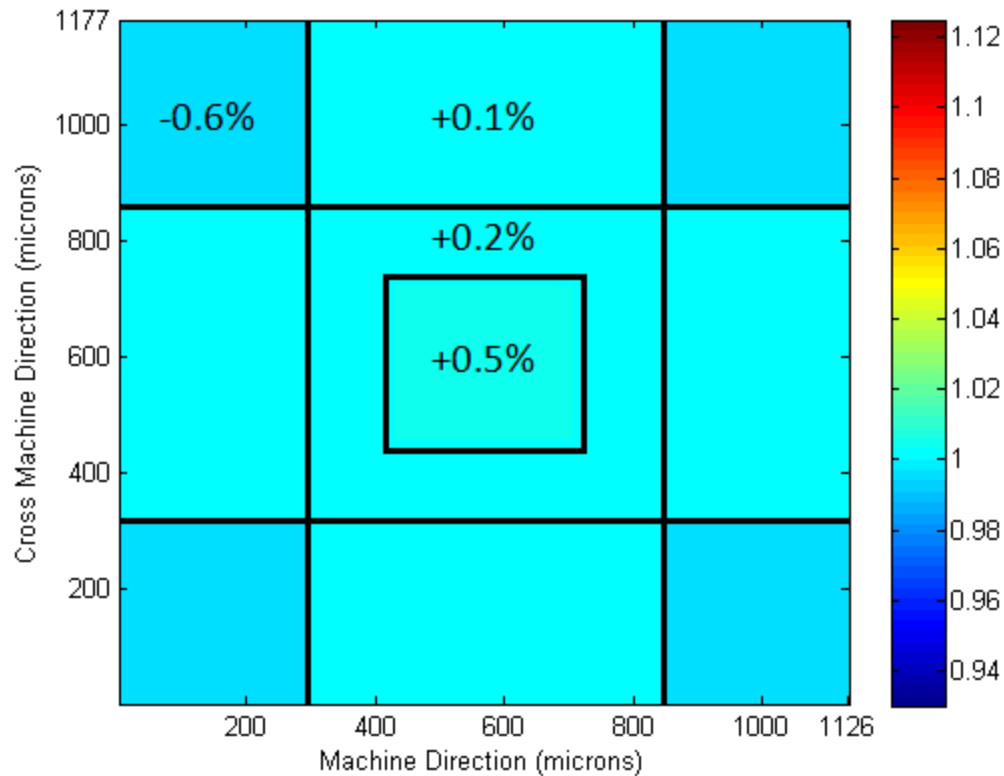
Figure 32: Top side PCC filler distribution under vacuum drainage with retention aids

It can be seen from Figure 32 that on the top side of the samples the knuckles contain 0.6% less filler material than the sample mean, the area formed over the threads contains 0.1% more, and the outer and inner opening regions contain 0.2% and 0.5% more filler material than the area average, respectively. These results represent a maximum difference between the knuckles and inner opening of 1.1%. This maximum difference was found to be 1.5% in the vacuum drained PCC samples that did not contain any retention aids. Thus, on the top side of the paper, the presence of retention aids was found to reduce the spatial variation in filler concentration by almost 30%. This difference was found to be statistically significant with the use of the t-test at a 95% confidence level.

The explanation of this result, as compared to the minimal effect of the retention aids on the wire side of the paper, is once again due to the difference in the flow field variations at different distances from the forming fabric. As previously stated, the bonds created by the retention aids are susceptible to strong hydrodynamic forces. At the wire side of the paper, where the flow field is dramatically different between the regions of the flow over an opening and a knuckle, the fibres experience large shear forces. However, at a distance from the forming fabric, where the top side of the paper is being formed, the discrepancies between flow velocities in different areas is less severe, and consequently the fibres on

the top side of the paper experience smaller shear forces during formation. Thus, the bond between filler material and fibres created by the retention aids is able to resist the distributing effects of the flow field to a greater extent on the top side, resulting in a more uniform filler distribution when retention aids are used.

Finally, as a control, the effect of retention aids on the distribution of PCC filler were investigated for the wire side of samples formed under gravity drainage. This was done to investigate how the retention aids affected distribution in a situation where the hydrodynamic forces are higher than on the top side of the paper, but lower than on the wire side during vacuum drainage. It was found that the maximum difference between the knuckles and inner opening zones is 4.3%.
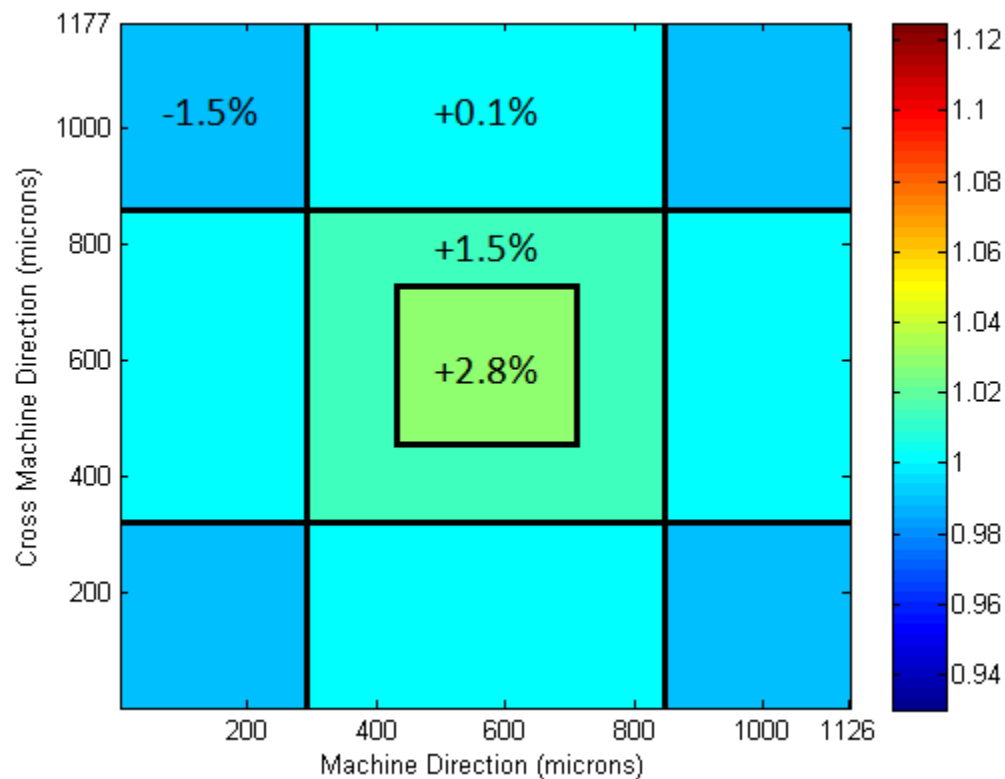
Figure 33: Wire side PCC filler distribution under gravity drainage with retention aids

The same result without retention aids was found to have a maximum distribution of 5.2%. The presence of retention aids on the wire side of the paper under gravity drainage therefore reduced the maximum filler distribution by approximately 17%. This effect is in line with the effects of the shear forces previously described by the vacuum results. Under gravity drainage, the shear forces acting on the filler particles are smaller than the forces during vacuum drainage, since the drainage velocity is lower. Consequently, less filler material is sheared from the pulp fibres and deposited elsewhere by the

water flow. The result is a noticeably more uniform filler distribution under gravity drainage, whereas there was no noticeable improvement in uniformity when retention aids were used with vacuum drainage.

3.4   Experiments with Industry Forming Fabric

The final set of experiments involved testing the filler distribution in paper samples made with a forming fabric used in industry. The fabric was a single layer, 1-4 broken twill weave, made by AstenJohnson. As outlined in section 2.5, it was identified that the fabric contains two distinct types of opening and 3 distinct knuckles. To describe the filler distribution in paper made with this fabric, the filler content in the paper formed over these 5 areas was calculated. The areas of interest in the forming fabric are shown in Figure 21. The analysis was done in the same way as in sections 3.1 – 3.3. The normalised intensity value was calculated as a representation of the relative concentration of filler material in each area of interest. These values were then averaged over a large number of samples to minimise the effects of the noise. The results, represented as a percentage above or below the sample mean, are summarised in Table 3.

Table 3: Normalised calcium intensity values in areas of paper formed with industry forming fabric

Region	Percentage of filler relative to sample mean
Opening I	+2.4%
Opening II	+3.4%
Knuckle I	-1.7%
Knuckle II	-1.8%
Knuckle III	-2.1%

It can be seen from the results in Table 3 that, like the general distribution found for the simplest forming fabric in sections 3.1 – 3.3, the areas of the paper formed over openings in the forming fabric contain more filler than the total sample mean, and the areas formed over knuckles contain less. Specifically, paper formed over the openings that are surrounded by the most uniform array of fabric strands (Opening II) contains the most filler material, with 3.4% more than the total mean; and the areas formed over the highest raised knuckles (Knuckle III) contain the least filler, with 2.1% less than the

average sample value. Thus, the largest discrepancy in filler concentration on the surface of the paper occurs between these two regions and is equal to a difference of 5.5%.

This result is particularly interesting when compared with the maximum distribution values calculated for paper of the same stock formed on the simple sinusoidal fabric. Both experiments were conducted with samples made from the same pulp suspension containing PCC filler and retention aids. Dewatering was done with an applied suction of 33.86 kPa. With the simple forming fabric, the maximum filler difference was 11.3%. Thus, the AstenJohnson fabric represents a reduction in the variability of the filler distribution of 51%. This number is extremely important, considering that one of the main purposes and selling points of a complex forming fabric is its ability to produce uniform paper. The comparison between these two cases shows, in a measurable way, how well this particular forming fabric is able to uniformly distribute the filler material on the surface of the final paper product.

CHAPTER 4 – CONCLUSIONS AND RECOMMENDATIONS FOR FUTURE WORK

4.1   Summary and Conclusions

A series of experiments were conducted to measure the distribution of filler material on the surface of paper, at the level of individual strands of the forming fabric, in both the machine and cross-machine direction. Paper samples were made with a laboratory hand sheet forming apparatus that was designed to simulate the drainage cause by suction boxes. The device allows the user to make samples with their choice of forming fabric and pulp suspension, as well as control the applied suction used for drainage. The purpose of the experiments was to measure how different properties of the pulp suspension, and of formation, affected the filler distribution in the resulting samples. In all cases, the suspension was prepared at 0.5% consistency, and the filler material constituted 40% of the dry material, by weight. The effect of changing the filler material, drainage rate, presence of retention aids, and type of forming fabric on the distribution of the filler material was observed on both the top and wire sides of the paper.

Filler distribution was measured in terms of relative concentration of filler material between pre-determined zones. The zones correspond to areas of paper formed above areas of interest in the forming fabric. These areas are the threads of the fabric, the knuckles, and the openings. One sample was taken to be one repeat pattern in the geometry of the forming fabric. The amount of filler material was calculated in each zone and normalised with the mean value for the sample. These values were used to represent the distribution of filler material across one repeat pattern. The majority of the deposition of filler material is associated with the pulp fibres; a very large variation in filler distribution arises solely from the variability in fibre deposition. However, it was found that a comparatively small, but repeated, variation in the filler concentration is due to the geometry of the forming fabric and the drainage flow field.

4.1.1   Effects of Filler Type

The effect of the type of filler material on the surface distribution was investigated using Precipitated Calcium Carbonate ($CaCO_3$) and Kaolin Clay $Al_2Si_2O_5(OH)_4$ filler. This series of experiments was conducted under gravity drainage to control the water removal rate for the samples. For both filler types, the distribution on the top and wire sides of the samples was analysed. It was found in all cases that, as

hypothesized, the areas of the paper formed over knuckles of the forming fabric contained the least amount of filler material, the area formed over threads contained about as much as the sample mean value, the outer area of the opening contained a higher amount than the threads, and the area of the sample with the most filler material was the inner opening.

- The maximum difference between zones was used as a measure for the level of non-uniformity; this value was the difference between the knuckles and inner opening in all cases.
- The maximum difference for samples made with PCC filler was found to be 5.2% on the wire side and 1.3% on the top side. The difference was found to be 11.2% on the wire side of the clay samples and 1.9% on the top side.
- The large difference in wire side distribution between the filler types is thought to be caused by electrostatic attraction between the filler material and the wood pulp fibres. PCC is cationic in distilled water, Kaolin is anionic, and pulp fibres are anionic [23, 27, 28]. The PCC is attracted to the fibres, resisting the effects of the flow field and creating a more uniform distribution. The opposite is true for Kaolin.
- Non-uniformity in the flow field is caused by the forming fabric geometry and this effect diminishes quickly with distance from the fabric and the buildup of the paper mat [53, 54]. Consequently, the top side distribution is considerably less pronounced than the wire side for both filler types. It was found that the top side distribution of clay was comparable to that of the PCC due to the uniform flow field and corresponding low shear stress at the top.

4.1.2 Effects of Drainage Rate

The effect of the dewatering rate on filler distribution was investigated by comparing the gravity drainage results with the distribution in samples formed when the water was removed by a vacuum suction of -33.86 kPa. This value was chosen for its high repeatability in the laboratory and its proximity to the pressure applied by industry suction boxes, which range from -15 to -60 kPa [13]. The same distribution pattern was found to be present as in the gravity drainage results: the centre of the opening contained the most filler, followed by the outer region of the openings, then the threads. The area of the paper formed over the knuckles contained the least filler.

- The maximum difference between the knuckles and inner opening with PCC filler was found to be 11.5% on the wire side and 1.5% on the top side. The maximum difference with clay filler was found to be 16.4% on the wire side and 2.0% on the top side.

- In general, it was found that an increase in dewatering rate increases the variation in filler concentration on the surface of the paper. With PCC filler, an applied suction of 33.86 kPa caused an increase in filler variation of 121% on the wire side and 15% on the top side from the gravity drainage results. For PCC filler, the variance increase was 46% on the wire side and 5% on the top side.

- The magnitude of the difference in the distribution between the two filler cases that was seen in the gravity drainage case was diminished with a larger applied suction. Under gravity drainage, the distribution variation of the clay filler was 2.15 times larger than the PCC filler, on the wire side of the paper. However, under vacuum drainage of 33.86 kPa, the clay filler distribution variation was found to be only 1.43 times as large as that of the PCC. This effect is thought to be attributed to the susceptibility of electrostatic bonds to hydrodynamic shear forces. As the drainage rate is increased, the shear forces acting on the filler material grow. The larger shear forces break more bonds between the PCC filler material and pulp fibres, which causes the filler distribution to more closely approximate that of the flow.

4.1.3   Effects of Retention Aids

The effect of retention aids on surface filler distribution was investigated by analysing samples made with PCC filler under vacuum and gravity drainage and comparing these results with the corresponding results without retention aids. The retention aids CPAM and silica were used, which work through the mechanisms of charge modification and macromolecular bonding.

- The samples behaved as expected under the effect of retention aids, retaining more filler material than the corresponding samples without retention aids.

- The maximum difference in filler content was found to be between the area of the sample formed over knuckles and the area in the centre of the opening, as with the other cases.

- The maximum difference was found to be 11.3% for the wire side vacuum case, which is within the experimental error of the 11.5% difference for pulp without retention aids.

- The maximum difference for the top side under vacuum drainage was found to be 1.1%, which is somewhat less than the 1.5% for the top side case without retention aids.

- The maximum difference for the wire side under gravity drainage was found to be 4.2%, slightly below the value of 5.2% for the sample with no retention aids.

- The bonds formed by retention aids are similar to electrostatic bonds in that they can be easily broken by the large hydrodynamic shear forces present in a non-uniform flow field [35, 40]. On the wire side of the paper under vacuum drainage, where the shear forces are highest, the bonds created by the retention aids are broken, allowing the filler material to essentially move as if no retention aids are present. Consequently the filler distribution on the wire side of the paper under vacuum drainage is almost unaffected by the presence of retention aids. In contrast, with gravity drainage and at the top side of the paper, where the shear forces are lower, the retention aid bonds are relatively unbroken and therefore the variance in filler distribution is smaller than without retention aids.

4.1.4 Effects of Forming Fabric

The effects of the forming fabric design on filler distribution were investigated by making a series of samples with a different forming fabric than the one used for the previous experiments. The samples were made to simulate paper made in industry as closely as possible, so retention aids and a vacuum drainage of 33.86 kPa were employed. These results were then compared with the corresponding results made on the original forming fabric. Previous experiments were conducted with a single layer forming fabric with the "1-over-1-under" design. The substitute fabric is also one layer but has a "4-over-1-under" design. The fabric is made by AstenJohnson and carries the part number X-061088092XCXCB. The normalised filler distribution was calculated for different knuckle and opening geometries.

- The maximum filler difference was found to be between the wholly symmetric opening and knuckle geometry. The normalised difference in filler content was equal to 5.5%.
- This difference represents a decrease in filler non-uniformity of about half (51%) when compared to the paper samples prepared under the same conditions on the 1-over-1-under style fabric.
- The 4-over-1-under fabric is considerably finer than the 1-over-1-under. The improvement in the uniformity in filler distribution is believed to be attributed to this fact. With a finer forming fabric, the fluctuations in areas of high and low filler concentration have a higher frequency but lower magnitude.

4.2   Strengths and Limitations of Research

The techniques employed to measure the distribution of filler material have been designed to give an accurate representation of the *relative* concentration of filler material between zones in a sample, not the *total* concentration value. This was done for two main reasons. EDX analysis was originally designed as a qualitative assessment tool; it has only recently become relevant in quantitative analysis with technological advancements. The probabilistic nature of the method makes it unfit to fully quantify the atomic make-up of a sample. It is, however, excellent for determining the general make-up of a region. Secondly, since the deposition is so random and many samples needed to be averaged to uncover a reliable trend, by calculating the relative concentration, it allowed for samples with a varying amount of total filler material to be compared directly.

The results are particularly useful for comparing the total distribution of filler material between zones for the various samples. It can clearly be seen that local filler concentration for the wire side clay results under vacuum drainage are less uniform than the wire side PCC under gravity drainage, for example. However, this data does not provide any information about which sample has more total filler material on its surface. Thus, the data are excellent for showing surface filler distribution but does not say anything about the total amount of filler material in one zone or the next.

4.3   Recommendations for Future Work

To further investigate the effects of pulp suspension and drainage characteristics on the resulting paper samples, there are a number of experiments that can be carried out using the same apparatus.

The work conducted in this thesis consisted largely of comparisons between two extremes to investigate the effects of certain drainage properties. For example, to measure the effects of drainage velocity on the filler distribution, experiments were conducted under gravity drainage, and under an applied suction of 33.86 kPa. Further experiments should be conducted to develop a relationship curve in two main areas.

- The effect of suction pressure on filler distribution could be measured in greater detail by analysing samples formed under a range of pressures. This way, plots could be developed for

paper samples with certain characteristics, showing how the filler distribution varies with water removal rate.

- Use a method like sheet splitting to examine the filler distribution in the x-y plane in the interior of the sample. Features of the forming fabric could be identified in the paper using the same pinhole approach. The sheet would then be split and the surface of the paper could be analysed in the same way to see the MD-CMD distribution in the middle of a sheet. If adequate accuracy was achieved, the same process could be repeated at various points throughout the thickness of the paper. This information would provide insight in how the distribution changes from the top to the wire side of the paper, and this could be correlated with numerical and experimental measures of the flow field at different distances from the forming fabric.

In a similar vein to the work done here, an investigation into the distribution of fine materials would likely provide great insight. Fines are larger and have less mobility than filler material. Compared to filler material, the likeliness of mechanical entrapment by larger pulp fibres would be increased, and the effects of the flow field on the redistribution of the fines would be diminished. An experimental procedure to investigate fine distribution, as outline by Dr. Mark Martinez, involves fractionation of the fine material from the fibres. The fines would then be treated with Bromine and reintroduced into the pulp suspension. The analysis could then proceed in the manner described in this work, but the EDX software would be set to map the presence of Bromine rather than an element found in the filler materials. Through image analysis techniques, the distribution of the fines could be mapped.

Further work with industry forming fabrics should be conducted. An analysis of the surface filler distribution of paper samples made on multilayer forming fabrics would be beneficial. The flow field becomes increasingly complex through a multi-layer fabric. Areas of high flow would have to be identified and related to the filler distribution. This research area has a large potential to quantify the effect of fabric geometry on filler uniformity.

It has become apparent, through the analysis of the top side of samples under various forming conditions, that a certain threshold exists that governs the movement of filler material in more uniform flow. It was peculiar to note that on the top side of the paper, the magnitude of the distribution was very similar for the gravity and vacuum drainage results. It is thought that there is a certain level of non-uniformity in the flow, above which the drainage rate has an effect on the distribution, but below which

it does not. An investigation into this effect, and the flow field that causes no filler re-distribution would

be of interest.

REFERENCES

[1] G. A. Smook, Handbook for pulp & paper technologists, Vancouver: Angus Wilde Publications, 2002.

[2] J. D. Peel, Paper Science and Paper Manufacture, Vancouver: Angus Wilde Publications, 1999.

[3] U. Haggblom-Ahnger, P. Pakarinen, M. Odell and D. Eklund, "Conventional stratified forming of office paper grades," *Tappi Journal,* vol. 81, no. 5, pp. 149 - 157, 1998.

[4] W. H. Griggs, "Use of fillers in papermaking," *Tappi Journal,* vol. 71, no. 4, pp. 77 - 81, 1988.

[5] R. G. Johnson, "1985 Alkaline Papermaking Seminar Notes," in *Tappi Press*, Atlanta, 1985.

[6] G. Gavelin, Paper Machine Design and Operation, Vancouver: Angus Wilde Publications, 1998.

[7] R. A. Bartlett, L. T. Bieglar, J. Backstrom and V. Gopal, "Quadratic programming algorithms for large-scale model predictive control," *Journal of Process Control,* vol. 12, no. 7, pp. 775 - 795, 2002.

[8] K. W. Britt and J. E. Unbehend, "Water removal during sheet formation," *Tappi Journal,* vol. 63, no. 4, pp. 67 - 70, 1980.

[9] R. Singh, S. Lavrykov and B. V. Ramarao, "Permeability of pulp fibre mats with filler particles," *Colloids and Surfaces A: Physicochemical and Engineering Aspects,* vol. 333, pp. 96 - 107, 2009.

[10] K. W. Britt, Handbook of Pulp and Paper Technology, New York: Van Nostrand Reinhold, 1970.

[11] S. Ramaswamy, "Vacuum Dewatering During Paper Manufacturing," *Drying Technology,* pp. 685-717, 2003.

[12] H. J. Bugge, "Forming Fabric of Double-Layer Type". Sweden Patent 4,611,639, 16 September 1986.

[13] P. Aslund and H. Vomhoff, "Dewatering mechanisms and their influence on suction box dewatering processes - A literature review," *Nord. Pulp and Paper Res. J.,* vol. 23, no. 4, pp. 389 - 397, 2008.

[14] K. Raisanen, "The effects of retention aids, drainage conditions and pretreatment of slurry on high vacuum dewatering: a laboratory study," in *Papermakers Conference 463 - 467*, San Francisco.

[15] W. B. Campbell, "The physics of water removal," *Pulp and Paper Magazine of Canada,* vol. 48, no. 3, pp. 103 - 109, 1947.

[16] C. Dong, D. Song, T. Patterson, A. Ragauska and Y. Deng, "Energy Saving in Papermaking through Filler Addition," *Ind. Eng. Chem. Res.,* vol. 47, no. 21, pp. 8430 - 8435, 2008.

[17] S. Yoon and Y. Deng, "Clay-Starch Composites and Their Application in Papermaking," *J. Applied Polymer Science,* vol. 100, no. 2, pp. 1032 - 1038, 2006.

[18] M. Karlsson, "Papermaking part 2: Drying," in *Tappi Press*, Atlanta, 2000.

[19] S. Park, R. A. Vendetti, H. Jameel and J. Pawlak, "Hard-to-remove Water in Cellulose Fibers Characterized by Thermal Analysis: A Model for the Drying of Wood-based Fibers," *Tappi Journal,* vol. 90, no. 6, pp. 10 - 16, 2007.

[20] R. Gill and W. Scott, "The relative effects of different calcium carbonate filler pigments on optical properties," *Tappi Journal,* vol. 70, no. 1, pp. 93 - 99, 1987.

[21] R. A. Gill, "Filler for Papermaking," [Online]. Available: http://www.specialtyminerals.com/fileadmin/user_upload/smi/Publications/S-PA-AT-PB-42.pdf . [Accessed 28 June 2012].

[22] M. Laufmann, M. Forsblom, M. Strutz and S. Yeakey, "GCC vs. PCC as the primary filler for uncoated and coated wood-free paper," *Tappi Journal,* vol. 83, no. 5, pp. 29 - 41, 2000.

[23] H. Murray and J. E. Kogel, "Engineered clay products for the paper industry," *Applied Clay Science,* vol. 29, no. 3, pp. 199 - 206, 2005.

[24] M. Cechova, "Stability of ground and precipitated CaCO3 suspensions in the presence of polyethylene oxide and kraft ligning," *Colloids Surf. A Physiochem. Eng. Asp. ,* vol. 141, no. 1, pp. 153 - 160, 1998.

[25] D. Siffert and P. Fimbel, "Parameters affecting the sign and magnitude of the electrokinetic potential of calcite," *Colloids Surf. A Physiochem. Eng. Asp. ,* vol. 11, no. 3, pp. 377 - 389, 1984.

[26] Š. Šutý and V. Lužáková, "Role of surface charge in deposition of filler particles onto pulp fibres," *Colloids Surf. A Physiochem. Eng. Asp.,* vol. 139, no. 3, pp. 271 - 278, 1998.

[27] A. Vanerek, B. Alince and T. V. d. Ven, "Collidal Behaviour of Ground and Precipitated Calcium Carbonate Fillers: Effects of Cationic Polyelectrolytes and Water Quality," *J. Pulp Paper Sci.,* vol. 26, no. 4, pp. 135 - 139, 2000.

[28] T. Herrington, A. Clarke and J. Watts, "The surface charge of kaolin," *Colloids and Surfaces,* vol. 68, no. 3, pp. 161 - 169, 1992.

[29] A. Vanerek, B. Alince and T. V. d. Ven, "Interaction of Calcium Carbonate Fillers with Pulp Fibres: Effect of Surface Charge and Cantionic Polyelectrolytes," *J. Pulp and Paper Sci.,* vol. 26, no. 9, pp. 317 - 322, 2000.

[30] Z. Yan and Y. Deng, "Cationic microparticle based flocculation and retention systems," *Chem. Eng. J.,* vol. 80, no. 1, pp. 31 - 36, 2000.

[31] W. Willets, "Factors Affecting Retention," *Pap. Trade J.,* vol. 101, no. 13, pp. 81 - 86, 1935.

[32] R. Pelton, B.D.Jordon and L. Allen, "Particle size distributions of fines and mechanical pulps and some aspects of their retention in papermaking," *Tappi Journal,* vol. 68, no. 2, pp. 91 - 99, 1985.

[33] R. Seth, "The measurement of significance of fines," *Pulp & Paper Canada,* vol. 104, no. 2, pp. 41 - 44, 2003.

[34] D. Solberg and L. Wȧgberg, "On the Mechanisms of GCC Filler Retention During Dewatering - New Techniques and Initial Findings," *J. Pulp Paper Sci.,* vol. 28, no. 6, pp. 183 - 192, 2002.

[35] B. Alince and F. Bednar, "Role of Cationic Polyacrylamide in Fiber-CaCO3 Pigment Interactions," *J. Appl. Polym. Sci.,* vol. 88, no. 10, pp. 2409 - 2415, 2003.

[36] D. Eklund and T. Lindstrom, Paper Chemistry: An Introduction, Finland: D.T. Paper Sci. Publications, 1991.

[37] T. v. d. Ven, "Theoretical Aspects of Drainage and Retention of Small Particles on the Fourdrinier," *J. Pulp Paper Sci.,* vol. 10, no. 3, pp. 57 - 63, 1984.

[38] M. Cadotte, M. Tellier, A. Blanco, E. Fuente, T. V. D. Ven and J. Paris, "Flocculation, Retention and Drainage in Papermaking: A Comparative Study of Polymeric Additives," *Canadian J. Of Ch. Eng.,* vol. 85, no. 2, pp. 240 - 248, 2007.

[39] J. Porubská, B. Alince and T. v. d. Ven, "Homo- and heteroflocculation of papermaking fine and fillers," *Colloids Sif. A Physiochem. Eng. Asp.,* vol. 210, no. 2, pp. 223 - 230, 2002.

[40] J. Shin, S. H.H., C. S. C., S. K.O. and M. S., "Highly branched cationic polyelectrolytes: Filler flocculation," *Tappi Journal,* vol. 80, no. 11, pp. 179 - 185, 1997.

[41] S. Roux, F. Feugeas, M. Bach, M. Fagon, C. Bettinger, S. Mourad and A. Cornet, "Determination of paper filler Z-distribution by low-vacuum SEM and EDX," *J. of Microscopy,* vol. 229, no. 1, pp. 44 - 59, 2008.

[42] A. Puurtinen, "Controlling filler distribution for improved fine paper properties," *Appita Journal ,* vol. 57, no. 3, pp. 204 - 209, 2004.

[43] M. Odell, "Paper Structure Engineering," *Appita Journal,* vol. 53, no. 5, pp. 371 - 377, 2000.

[44] A. Puurtinen, "A laboratory study on the chemical layering of WFC base paper," *Professional*

Papermaking, vol. 1, no. 1, p. 22, 2003.

[45] J. Bristow and N. Pauler, "Multilayer structure in printing papers," *Svensk Papperstidn,* vol. 86, no. 2, 1993.

[46] A. C. Mangin, P. Valade, J. Beland, M. Chartier and K. MacGregor, "The influence of underlying paper surface structure on missing dots in gravure," in *23rd Research Conference of IARIGAI*, Paris, 1995.

[47] H. Fordsmand, T. Maloney, J. Kananen, J. Kekkonen and C. Chen, "The Effect of Filler Distribution on Gravure Printability of SC Paper," in *JPGA Conference*, Cincinnatti, 2006.

[48] S. Modgi, M. McQuaid and P. Englezos, "SEM/EDX analysis of Z-direction distribution of mineral content in paper along the cross-direction," *Pulp & Paper Canada,* vol. 107, no. 5, pp. 48 - 51, 2006.

[49] D. Ormerod, G. Simon and D. Gibbon, "Paper mill additive and contaminant distribution mapping using energy dispersive X-ray analysis," *Tappi Journal,* vol. 71, no. 4, pp. 211 - 214, 1988.

[50] Z. Szikla and H. Paulapuro, "Z-directional distribution of fines and filler material in the paper web under wet pressing conditions," *Pap. Puu,* vol. 68, no. 9, p. 654, 1986.

[51] B. Radvan, "Forming of the paper web," in *Handbook of Paper Science*, Elsevier Scientific Publishing, 1982, p. Ch. 4.

[52] H. Tanka, "How retention aids change the distribution of filler in paper," in *Tappi Papermakers Conference*, 1982.

[53] H. Peng, "PIV Measurements of flow through forming fabrics," University of British Columbia, Vancouver, 2001.

[54] A. Vakil, S. Green and A. Olyei, "Three-dimensional geometry and flow field modeling of forming fabric," *Nordic Pulp and Paper Research J.,* vol. 24, no. 3, pp. 342 - 350, 2009.

[55] H. Bennis, R. Benslimane, S. Vicini, A. Mairani and E. Princi, "Fibre width measurement and qualification of filler size distribution in pape-based materials by SEM and image analysis," *J. of Electron Microscopy,* vol. 59, no. 2, pp. 91 - 102, 2010.

[56] R. Allem, "Characterization of Paper Coatings by Scanning Electron Microscopy and Image Analysis," *J. Pulp Paper Sci.,* vol. 24, no. 10, pp. 329 - 336, 1998.

[57] P. J. Goodhew, F. J. Humphreys and R. Beanland, Electron microscopy and analysis, New York: Taylor and Francis, 2001.

[58] J. Goldstein, Scanning Electron Microscopy and X-ray Microanalysis, New York: Kluwer Acadmeic/Plenum Publishers, 2003.

[59] R. Egerton, Physical Principles of Electron Microscopy, New York: Springer, 2005.

[60] R. "Van Greiken" and A. Markowicz, Handbook of X-Ray Spectrometry, New York: Marcel Dekker Inc., 1993.

[61] R. Jenkins, R. Gould and D. Gedcke, Quantitative X-ray Spectrometry, New York: Marcel Dekker Inc, 1995.

[62] J. Russ, Fundamentals of Energy Dispersive X-ray Analysis, Toronto: Butterworths & Co Ltd., 1984.

[63] D. Gibbon, G. Simon and R. Cornelius, "New electron light optical techniques for examing papermaking," *Tappi Journal,* vol. 72, no. 10, pp. 87 - 91, 1989.

[64] M. Martinez, "MECH 450 - Approach Flow," University of British Columbia, Vancouver, 2009.

[65] J. Montgomery, S. Green and A. Vanerek, "Effect of applied vacuum box suction on overall retention in hand sheet forming," *Nordic Pulp and Paper Research Journal,* vol. 25, no. 4, pp. 463 - 472, 2010.

[66] S. Green, Z. Wang, T. Waung and A. Vakil, "Simulation of the flow through woven fabrics," *Computers & Fluids,* vol. 37, pp. 1148 - 1156, 2008.

APPENDICES

Appendix A – Determination of Number of Frames

As explained in the introduction and method sections, when a sample is scanned with the EDX detector, there is only a small percent chance that an element of interest will absorb the incident x-ray and release a suitable characteristic x-ray. For this reason, the more times a sample area is scanned, the more accurate the elemental map will be. However, scanning the sample takes time, and I was severely limited by the time I was able to use the SEM and EDX equipment. Thus, it was imperative that I determine the optimal scan length that balances accuracy and efficiency. To length of the scan is measured in frames. One frame represents a single pass of the EDX detector over the sample and takes about 5 seconds to complete. To determine the ideal exposure time for one experiment, a sample was scanned for 5 different durations: 10, 20, 60, 120, and 360 frames. The elemental maps of these 5 cases are shown below.
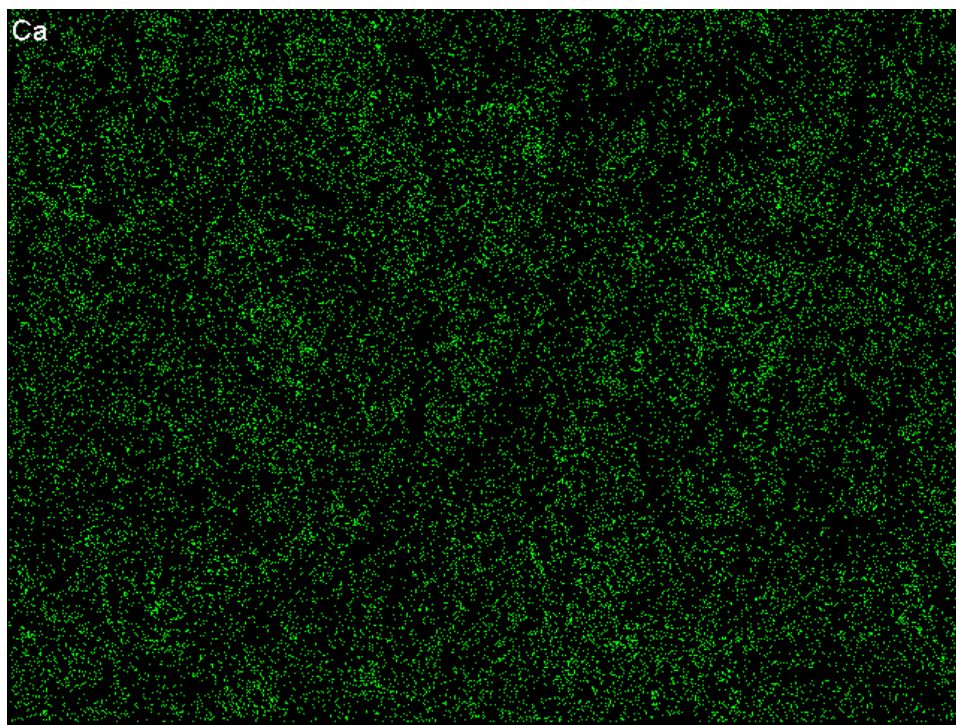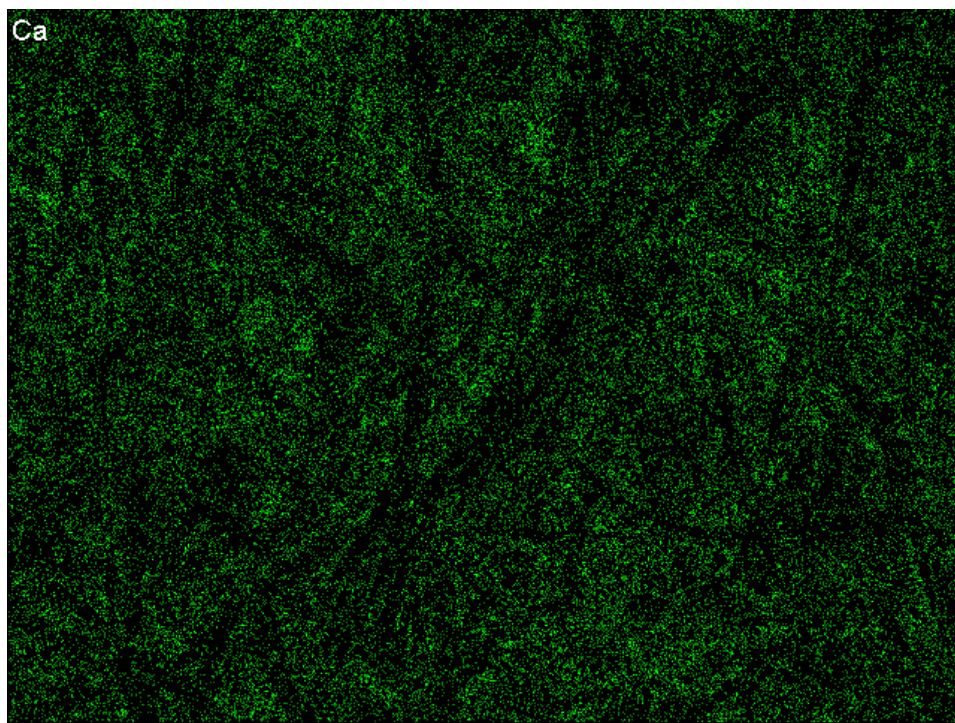

Figure 34: Sample area after 10 frames
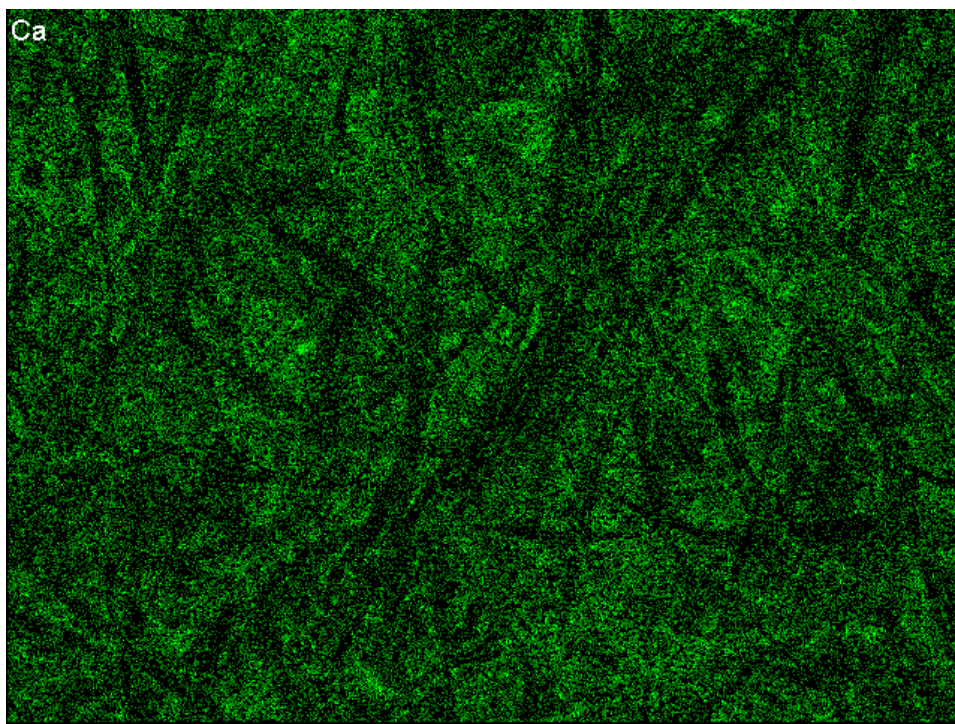
Figure 35: Sample area after 20 frames

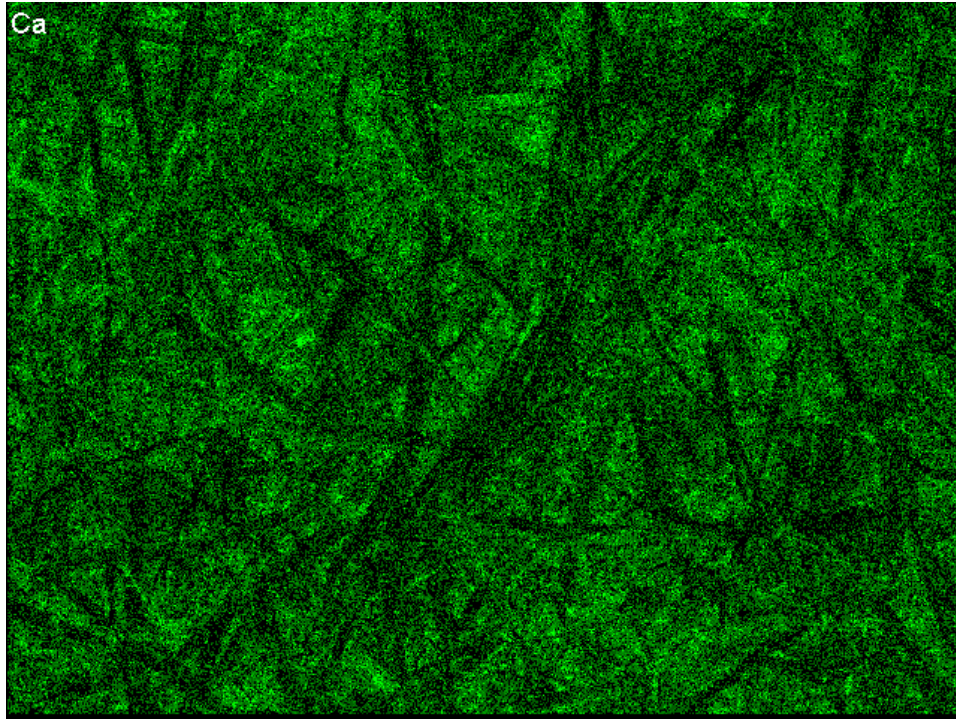*Figure 36: Sample area after 60 frames*
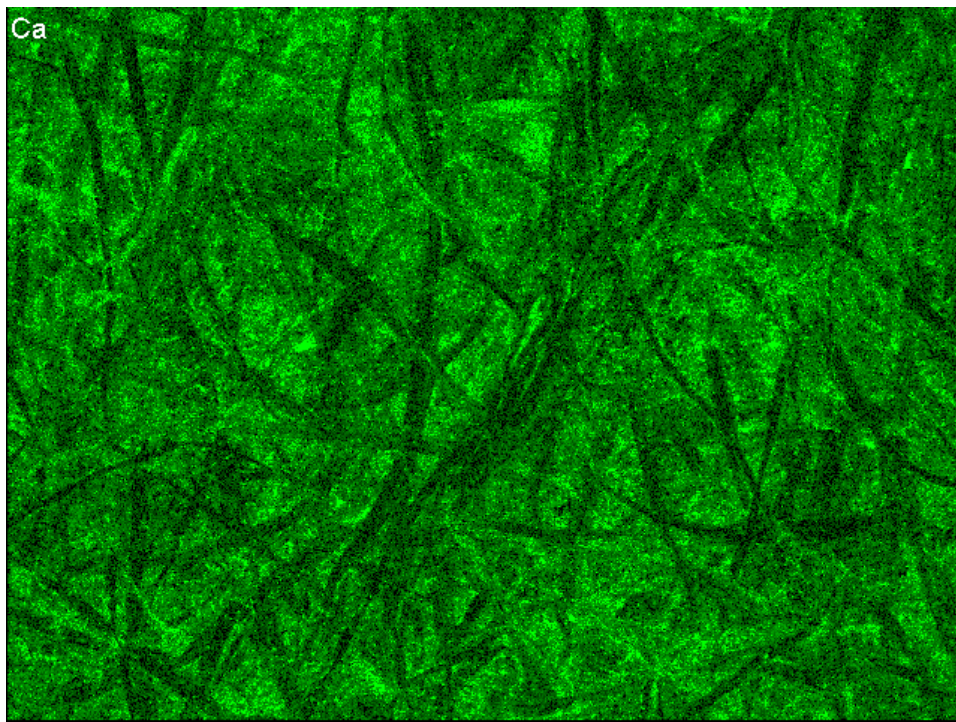
Figure 37: Sample area after 120 frames

Figure 38: Sample area after 360 frames

As can be seen in the above 5 figures, the longer the sample is scanned, the brighter the average pixel – which indicates a greater presence of calcium. This makes sense, considering the EDX will detect more calcium the longer it is allowed to scan. The map constructed from 360 frames took 30 minutes to be put together. This scan length is far too long for my purposes, but it is the most accurate of the 5 shown here. Logically, as the EDX is allowed to scan for more time, it will construct an increasingly accurate picture of the location and density of the calcium atoms. Thus, to determine the accuracy of the other time length scans, the normalized intensity value was calculated for each zone (from the zoning pattern in Figure X of the method) and these values were compared with the results from the 360 frame case. Essentially, the error was calculated for the 10, 20, 60, and 120 frame scans based on their difference with the 360 frame scans. These results are summarized below in Table 4.

Table 4: Determination of error for variable length scans

Sample	Mean Percent Error
10 Frames	5.21
20 Frames	3.39
60 Frames	2.54
120 Frames	1.53
360 Frames	0

For several reasons, the scan length of 60 frames was chosen as the standard for the experiments. First, the mean error in each zone of the sample, in comparison with the 360 frame case, is 2.54 percent. The error for the 20 frame case is 33% higher than the 60 frame case, while the error for 120 frames is 44% less. Visually, the 60 and 120 frames offer a much better representation of the distribution than the 20 frame result. The Calcium pixels have enough count to really develop depth between the different concentration areas. For this reason it was decided to choose between 60 and 120 frames. With a scan length of 60 frames, it was possible to scan 12 different samples in a 2 hour time block in the microscope lab (maximum length of time allowed), while it was only possible to scan 8 samples at 12-frames/sample. It was determined that at a rate of 12 samples per session, the work would progress at a meaningful rate, while 8 samples per session was too slow. The added number of samples possible to collect at 20 frames per sample was not necessary since it would not have been possible to complete the analysis between sessions fast enough to keep pace.

To fully justify the use of 60 frames per sample, the standard deviation of the error values was calculated to be 0.097, and the standard deviation of the data collected for a set of 60 frame samples is

0.149. Thus the sampling error is less than the random fluctuations of the data, which further supports the decision to use a scan length of 60 frames for the experiments.

Appendix B – Classification of Zones in AstenJohnson Forming Fabric

Within one repeat pattern of the 4-over-1-under forming fabric used in the experiments of section 3.4, there are a wide variety of knuckles and openings. This presented a challenge compared to the original 1-over-1-under fabric. In the plan weave forming fabric, the geometry of the knuckles is all the same, so the flow over every knuckle, strand, and opening is identical. Thus, the results for each zone could be average. However, with the industry fabric, the geometry of the knuckles differed throughout the repeat pattern, which leads to different regions experience slightly different flow patterns. If one was to average the results for all these areas, certain intricacies of the filler distribution caused by different flow patterns would be eliminated.

It can be seen that certain knuckles are the same, but in different orientations, and the same can be said for the openings. A method was devised to classify the knuckles based on the over/under orientation of the cross machine direction threads in each cardinal direction. An example is shown below.
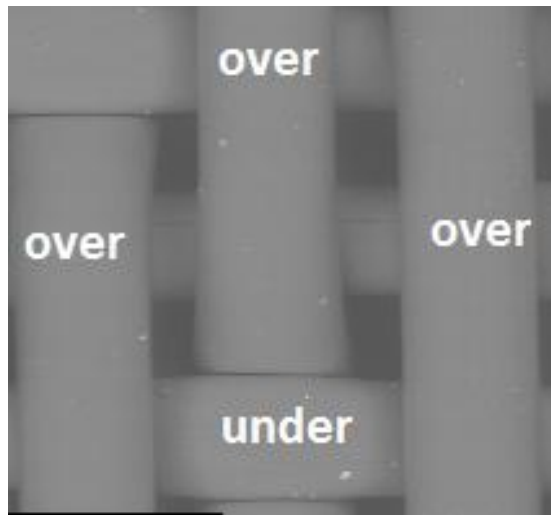

Figure 39: Knuckle with "under" thread in south position

In this image the central knuckle is being classified. It can be seen that the surrounding CMD threads to the north, east, south, and west are labelled based on whether they are on the top or bottom side of the fabric. This pattern also exists where the "under" thread is in the northern position. These two arrangements would produce the same flow field so the results are averaged together.

The second type of knuckle has the "under" thread in either the west or east position. These two permutations produce the same field and results from the two are averaged. Examples are shown below.
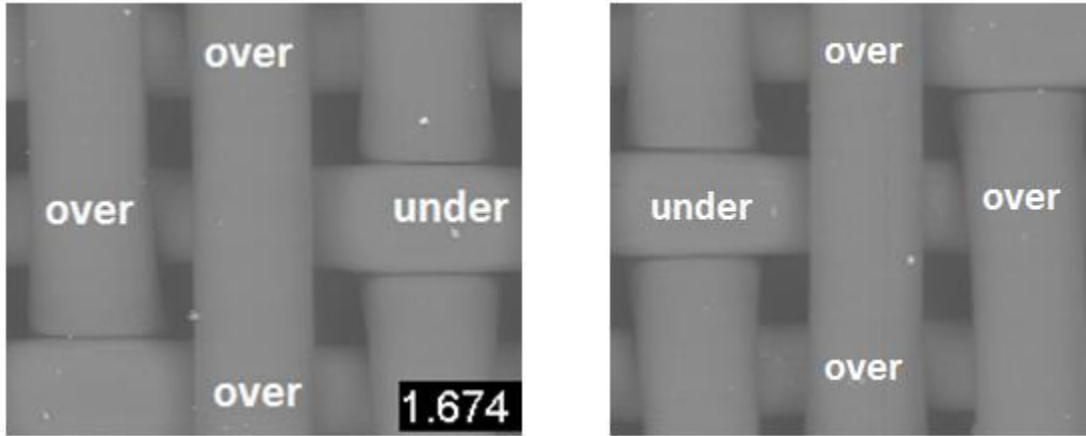

Figure 40: Variation of knuckle with "under" thread in east or west position

The third type of knuckle has the "under" thread in the centre and is surround by all over threads.
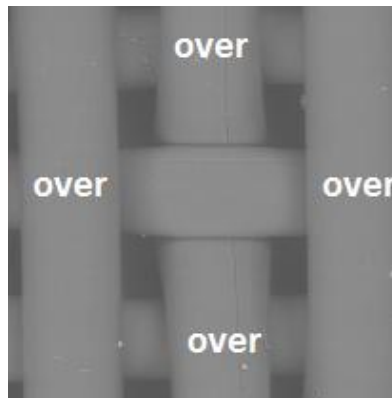

Figure 41: Centred knuckle variation

This process was repeated for the CMD threads surrounding an opening. It was found that two types of openings exist, which can be seen below. The data for all similar types of openings was group together to determine the filler concentrations shown in section 3.4.
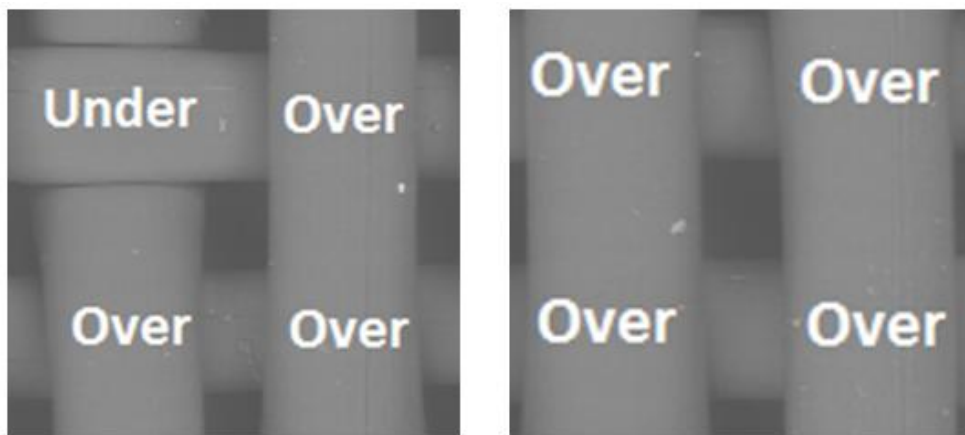
Figure 42: The two varieties of openings

Appendix C – Statistical Significance of Filler Concentration Values

The statistical significance of the filler concentration values in each zone needed to be verified, at a confidence level of 95%. This was done by conducting a Student's t-test comparing the concentration values for the zone with the concentration values for the entire sample. The null hypothesis, H_0, was said to be that there is no statistical difference between the values. Thus by disproving the null hypothesis, a statistical difference is established. H_0 does not hold if the absolute value of the experimental t value is greater than the theoretical t value. In the Excel Data Analysis package, this mean that "|t-stat|" must be larger than "t Critical two-tail". It can also be said that the result is significant on a 95% confidence interval if $p < 0.05$. In Excel, "P(T<=t) two tail" must be less than 0.05.

Sample analyses of the significance of the data for Knuckle 1 and the Inner Opening zones for the wire side clay gravity results are shown in Figure 43.

	Knuckle 1	Sample Mean
Mean	19.515	21.675
Variance	41.345	52.187
Observations	32	32
Pearson Correlation	0.964	
Hypothesized Mean Difference	0	
df	31	
t Stat	-6.133	
P(T<=t) one-tail	0.000	
t Critical one-tail	1.696	
P(T<=t) two-tail	0.000	
t Critical two-tail	2.040	

	Inner Opening	Sample Mean
Mean	22.967	21.675
Variance	68.555	52.187
Observations	32	32
Pearson Correlation	0.946	
Hypothesized Mean Difference	0	
df	31	
t Stat	2.657	
P(T<=t) one-tail	0.006	
t Critical one-tail	1.696	
P(T<=t) two-tail	0.012	
t Critical two-tail	2.040	

Figure 43: T-test results for K1 (left) and Inner Opening (right) of wire side clay gravity drainage sample

As can be seen in Figure 43, the absolute magnitude of the "t Stat" value for both Knuckle 1 and the Inner opening is greater than the corresponding "t Critical two-tail" value. This meets the criteria for a statistically significant result, allowing the confident assertion that the mean zone concentration value is above or below the sample mean. This test was repeated for all zones in the results section.